Geochemistry Geophysics Geosystems G3
AN ELECTRONIC JOURNAL OF THE EARTH SCIENCES
Published by AGU and the Geochemical Society

*Article*
Volume 8, Number 9
29 September 2007
Q09016, doi:10.1029/2007GC001712
ISSN: 1525-2027



# Seamount morphology in the Bowie and Cobb hot spot trails, Gulf of Alaska

**Jason D. Chaytor**
*College of Oceanic and Atmospheric Sciences, Oregon State University, 104 COAS Admin. Building, Corvallis, Oregon 97331, USA*

*Now at Department of Geology and Geophysics, Woods Hole Oceanographic Institution, MS #24, Woods Hole, Massachusetts 02543, USA (jchaytor@whoi.edu)*

**Randall A. Keller**
*Department of Geosciences, Oregon State University, 104 Wilkinson Hall, Corvallis, Oregon 97331, USA*

**Robert A. Duncan**
*College of Oceanic and Atmospheric Sciences, Oregon State University, 104 COAS Admin. Building, Corvallis, Oregon 97331, USA*

**Robert P. Dziak**
*Cooperative Institute for Marine Resources Studies, Oregon State University/National Oceanic and Atmospheric Administration, HMSC, Newport, Oregon 97365, USA*

[1] Full-coverage multibeam bathymetric mapping of twelve seamounts in the Gulf of Alaska reveals that they are characterized by flat-topped summits (rarely with summit craters) and by terraced, or step-bench, flanks. These summit plateaus contain relict volcanic features (e.g., flow levees, late-stage cones, and collapse craters) and as such must have been constructed by volcanic processes such as lava ponding above a central vent, rather than by erosion above sea level. The terraced flanks are composed of a sequence of stacked lava deltas and cones, probably tube-fed from a central lava pond, a morphology which is suggestive of long-lived, stable central lava sources and low to moderate eruption rates, indicative of significant time spent above a hot spot outlet. Most of these seamounts have summit plateaus surrounded, and cut into, by amphitheater headwall scarps, and flanks that are scarred by debris chutes, but lack visible debris accumulations at their base. We interpret the lack of blocky debris fields as evidence that the slope failures are mainly small-scale debris flows, rather than large-scale flank collapses. However, we cannot rule out the possibility that large flank-collapse blocks from early in the histories of these seamounts are now hidden beneath the thick glacio-fluvial fan deposits that cover the Gulf of Alaska seafloor. These slope failure features become smoother and longer and increase in size and abundance with increasing age of a seamount, suggesting that slope failure processes continue long after volcanic activity ceases.

**Components:** 12,167 words, 14 figures, 1 table.

**Keywords:** bathymetry; slope stability; sea level; submarine volcanism.

**Index Terms:** 3045 Marine Geology and Geophysics: Seafloor morphology, geology, and geophysics; 8427 Volcanology: Subaqueous volcanism; 3070 Marine Geology and Geophysics: Submarine landslides.

**Received** 6 June 2007; **Revised** 26 July 2007; **Accepted** 7 August 2007; **Published** 29 September 2007.

Chaytor, J. D., R. A. Keller, R. A. Duncan, and R. P. Dziak (2007), Seamount morphology in the Bowie and Cobb hot spot trails, Gulf of Alaska, *Geochem. Geophys. Geosyst.*, *8*, Q09016, doi:10.1029/2007GC001712.

## 1. Introduction

[2] Linear chains of age-progressive seamounts aligned with the direction of plate motion are usually attributed to sublithospheric hot spots that create volcanic trails on a lithospheric plate as it passes over a focus of melting [*Wilson*, 1963]. The discontinuous chains of seamounts stretching across the Gulf of Alaska (Figure 1) are broadly age-progressive (younging to the southeast) and aligned with the direction of motion of the Pacific Plate [*Morgan*, 1972]. A hot spot origin is suggested for these seamount chains, but the ages of many edifices are unknown, and some of the known ages are out of sequence [*Silver et al.*, 1974; *Dalrymple et al.*, 1987]. Also, the compositions of the volcanic rocks on these seamounts are unusual in that they lack the distinctive radiogenic isotopic signatures of most hot spots [*Hegner and Tatsumoto*, 1989; *Desonie and Duncan*, 1990; *Allan et al.*, 1993; *Cousens*, 1996; *Keller et al.*, 1997]. These unusual aspects of the geochronology and geochemistry of the Gulf of Alaska seamounts have called into question the validity of the hot spot-mantle plume model for these seamounts [*Smoot*, 1985; *Dalrymple et al.*, 1987; *Allan et al.*, 1993]. A set of weak mantle plumes that are thermally buoyant, rather than compositionally buoyant, could explain the discontinuous nature and anomalous isotopic compositions of these seamount chains [*Desonie and Duncan*, 1990], though not the out-of-sequence ages. We are studying the volcanic histories of the Gulf of Alaska seamounts to understand how and why they formed and for how long they were volcanically active. These seamounts provide an excellent record of prevailing tectonic and volcanic processes within the Gulf of Alaska for the last 30 million years. While the gross relief and shape of some of these undersea mountains have been known for some time [e.g., *Chase et al.*, 1970; *Smoot*, 1981, 1985], their morphology, and hence the volcanic and tectonic processes responsible for their formation and subsequent modification, were largely unknown. A separate paper (R. Keller et al., manuscript in preparation, 2007) describes the geochemistry and geochronology of rocks recovered from most of the seamounts described herein.

[3] We present full-coverage multibeam swath bathymetric maps of twelve Gulf of Alaska seamounts, with additional partial coverage maps of several minor seamounts, all from beyond the immediate near-ridge environment. Six major seamounts from the Kodiak-Bowie Seamount Chain are described, including Bowie, Denson, Dickins, Welker, Pratt, and Giacomini seamounts; and six from the Cobb Seamount chain, including Cobb, Warwick, Scott, Murray, Patton, and Marchand (Figure 1). Additionally, multibeam maps of portions of several major abyssal plain channel systems acquired incidentally during mapping of the Kodiak-Bowie seamount chain reveal ongoing deep-sea fluvial processes, some of which affect the seamounts, and vice versa.

[4] Many of the seamounts described here are flat-topped, and could be called guyots, but we use the more generic term of seamount to avoid confusion with the wave-eroded coral-topped guyots of the southern Pacific. There is considerable evidence that the flat tops of the Gulf of Alaska seamounts were formed volcanically, and with the exception of Cobb Seamount, there is no evidence that these seamounts were ever at the sea surface.

## 2. Geologic Setting

[5] The Gulf of Alaska Seamount Province within the northeast Pacific Ocean encompasses an area extending from the Explorer-Juan de Fuca Ridge offshore Washington and British Columbia to the Aleutian Islands. This region contains over 100 distinct seamounts over 1000 m tall, although only a small fraction of the seamounts within the gulf are currently named.

[6] Two dominant seamount chains are present within the region, the Kodiak-Bowie seamount chain (referred to as the Pratt-Welker seamount chain by *Turner et al.* [1980] and *Lambeck et al.* [1984]) and the Cobb seamount chain (part of which is also known as the Cobb-Eickelberg chain [*Clouard and Bonneville*, 2005; *Desonie and Duncan*, 1990]). These seamounts sit atop seafloor

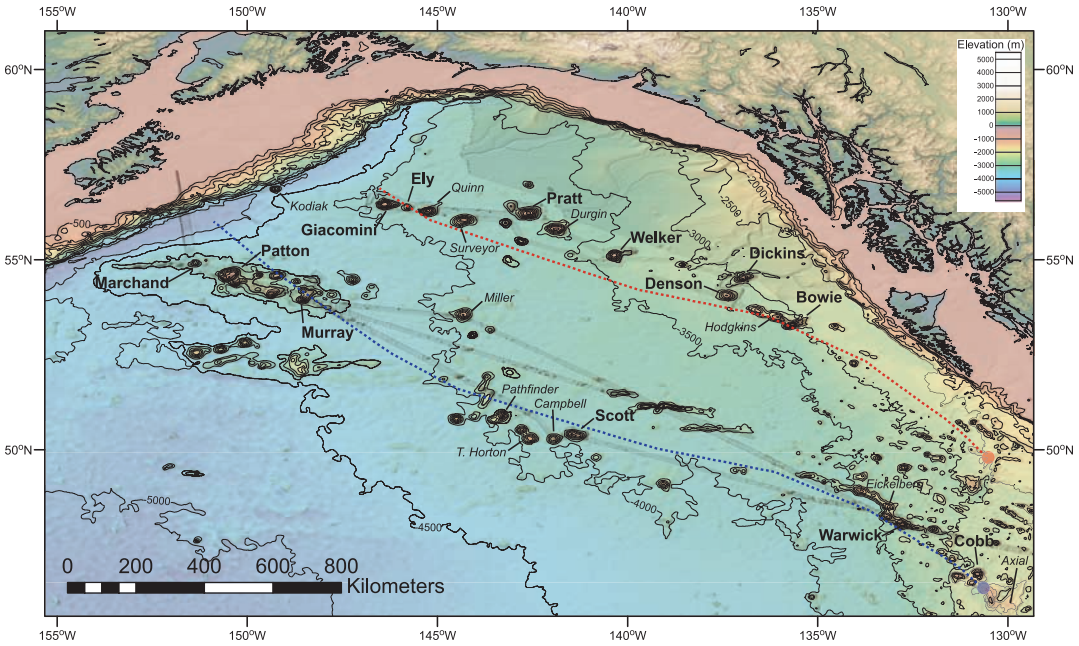


**Figure 1.** Bathymetric map of the Gulf of Alaska showing the location of major seamounts of the region and the absolute plate motion (APM) tracks for the Kodiak-Bowie and Cobb seamount chains from *Wessel et al.* [2006]. The approximate locations of the Cobb (blue circle) and Bowie (red circle) hot spots are also shown. The contour interval is 500 m. Bathymetry compilation contains satellite altimeter data from *Smith and Sandwell* [1997] and multibeam data from Atlantis cruises AT3-36, AT7-15, AT7-16, and AT11-15, Law of the Sea mapping cruises KM0514-1 and KM0514-2 [*Gardner and Mayer*, 2005], and National Ocean Service (NOS) surveys H10996 and H10999 [*Herlihy*, 2000].

ranging from magnetic chron 2A, to chron 19 [*Atwater and Severinghaus*, 1989], equivalent to crustal ages between 3 and 43–44 Ma, respectively.

[7] Fourteen major and numerous minor seamounts comprise the Kodiak-Bowie chain, which stretches from Kodiak Seamount just seaward of the Aleutian Trench, 900 km southeast to Bowie Seamount off the Queen Charlotte Islands (Figure 1). For the most part, these seamounts are age progressive, from Bowie, the youngest, at $\geq$0.7 Ma to Kodiak at 24 Ma and reflect movement of the Pacific plate over the Bowie hot spot [*Turner et al.*, 1973, 1980]. Out-of-sequence ages of some seamounts such as Denson (18.2 Ma [*Turner et al.*, 1980]) suggest that not all the seamounts within the chain formed over a hot spot, but possibly at the nearby ridge, a conclusion supported by the bathymetry presented here.

[8] The Cobb seamount chain extends from Marchand Seamount (26 Ma (R. Keller et al., manuscript in preparation, 2007)) just seaward of the Aleutian trench, through the Patton-Murray Seamount Platform and the Cobb-Eickelberg seamount chain, to Axial Seamount, the current location of the Cobb hot spot on the Juan de Fuca Ridge [*Desonie and Duncan*, 1990]. Like the Kodiak-Bowie chain, some out-of-sequence ages are found in the Cobb chain, suggesting either unusually late rejuvenated volcanism, a mix of ridge and hot spot generated seamounts [*Desonie and Duncan*, 1990], or a shift in the location of the Juan de Fuca ridge [*Dalrymple et al.*, 1987].

[9] Deep-sea sediment fans and associated leveed channels play a dominant role in shaping the seafloor morphology of the greater Gulf of Alaska, and as such, the morphology seen at the base of the seamounts in the region. Extensive Cenozoic sedimentation has buried much of the basement relief throughout the gulf with the individual seamount chains dividing the region into three abyssal plains, the Aleutian, Alaskan and Tufts abyssal plains (Figure 2) [*Hurley*, 1960; *Stevenson and Embley*, 1987]. The seamounts within this study lie within and at the boundaries of the Alaskan and Tufts Abyssal Plains, which themselves are composed of numerous deep-sea fan complexes. Dominant among these are the Surveyor and Baranof Fans (Figure 2) [*Stevenson and Embley*, 1987], which are composed of Eocene to present turbidite deposits derived from intense glacial erosion of mountain belts that bound the gulf. Sediment thickness

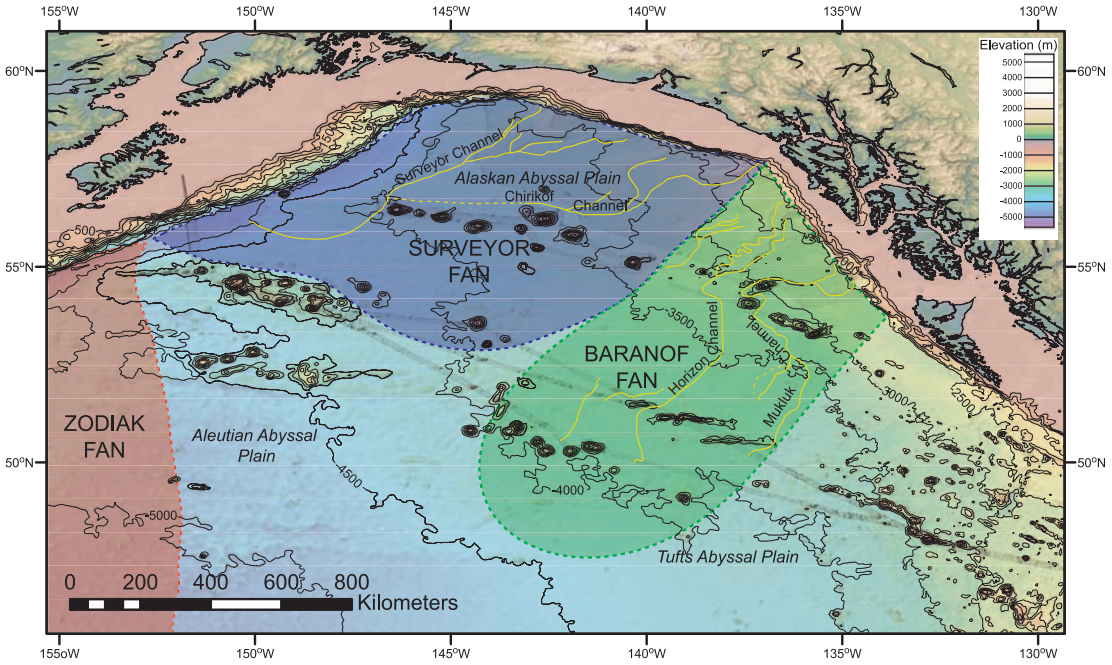


**Figure 2.** Major fan bodies (Zodiak, red; Surveyor, blue; Baranof, green), abyssal plains, and channel systems (marked in yellow; adapted from *Stevenson and Embley* [1987]) of the Gulf of Alaska that interact with the seamounts described in this study.

values within these bodies range from between 0.2 km and 3 km [*Winterer*, 1989], increasing to as much as 6 km in places [*Stevenson and Embley*, 1987]. The most recent phase of deposition within the Surveyor and Baranof fans is represented by extensive fan-body turbidite channels such as the Mukluk, Surveyor and Horizon channels (Figure 2). In some cases these channels are found to directly influence the morphology at the base of seamounts, and in others the direction and morphology of channels appear to be influenced by the presence of the seamounts. Several excellent examples of this can be seen in Figure 2, with the direction of the Mukluk Channel changing to account for the presence of Dickins and Denson seamounts directly within its downslope path. The southern end of the Surveyor Channel is controlled by the Patton Seamount complex, which forces the channel to turn north and enter the Aleutian Trench.

## 3. Methods

[10] Detailed high-resolution bathymetric and backscatter surveys used in this study were collected using the SeaBeam 2112 system during three cruises in 1999, 2002, and 2004 aboard the R/V *Atlantis*. The SeaBeam 2112 is a 12 kHz deep-water swath sonar system providing co-registered bathymetric soundings and backscatter intensity information, geo-located with positioning information from the Trimble Tasman P-Code GPS and corrected for vessel motion by inputs from a Datawell Hippy vertical reference unit (VRU). Sound velocity profiles were derived from expendable bathy-thermograph (XBT) casts on arrival at each seamount and applied to the bathymetry during acquisition. Subbottom data were acquired using a hull mounted 3.5 kHz Knudsen 320BR echosounder. Additional multibeam bathymetry covering Bowie and Hodgkins seamounts was collected by NOAA National Ocean Service in 2000 using a combination of Reson SeaBat 8101, SeaBeam/Elac 1180, and SeaBeam/Elac 1050D MkII mapping systems installed on the NOAA Ship Rainier and its launches [*Herlihy*, 2000]. Multibeam data for Cobb Seamount was collected in 2000 using the SeaBeam 2112 system installed on the R/V *Ronald H. Brown* [*Bobbitt et al.*, 2000].

[11] Initial data editing and processing were carried out at sea following acquisition using the MB-System multibeam bathymetry processing software packages [*Caress and Chayes*, 1996]. Additional data editing was performed prior to final map creation, which became critically important for seamounts such as Patton for which data were collected over

multiple years. Maps of the backscatter date produced following this processing stage showed the data to be of limited use largely because of a survey geometry favoring the collection of bathymetric information, and as such, the backscatter data were not used in the final interpretation of seamount morphologies. Final bathymetric maps are presented at a nominal pixel resolution of 100 m × 100 m. Morphological interpretation was carried out through three-dimensional visualization using IVS Fledermaus software. Summary statistical information about each seamount, including minimum and maximum depths, average slope values, and seamount area and circumference was obtained using both Fledermaus and ESRI ArcGIS. Depths are reported in meters below sea level and are uncorrected with respect to tide due to the inherent range resolution error of the system at deeper depths and the difficulty in determining such a correction at large distances from land.

## 4. Seamount Geology and Morphological Observations

[12] Each seamount in this study is morphologically distinct, so we describe them individually, with emphasis on overall edifice shape, a detailed description of volcanic features and constructional morphology where apparent, and evidence for slope failures of various scales. In general, these seamounts fall into two broad morphologic types, (1) round, flat-topped "guyots" and (2) linear, narrow and steeply sloped ridges, although in some cases slope failures have severely altered their shapes. The significance of these two morphological types will be addressed in the discussion. General parameters that pertain to each of the seamounts described in the following section and additional ones for which sufficient data exists for simple description are listed in Table 1.

### 4.1. Kodiak-Bowie Seamount Chain

#### 4.1.1. Bowie

[13] Bowie Seamount lies off the Queen Charlotte Islands near the southeast end of the Kodiak-Bowie chain. Its location and young age (0.075 to 0.7 Ma; Table 1) have been used to infer that it is near the current location of the Bowie hot spot [*Turner et al.*, 1980], although others place the hot spot farther southeast under the Tuzo Wilson Knolls [*Chase*, 1977]. Multibeam bathymetry [*Herlihy*, 2000] shows Bowie as a semi-linear ridge-like seamount composed of a main edifice, with a ~20 km-long NE-trending sharp linear ridge projecting from its northern slope (Figure 3). A flat, narrow summit plateau at a depth of approximately 235 m caps the main edifice. Several peaks up to 200 m tall are found on the summit plateau, the shallowest of which comes to within 34 m of the sea surface.

[14] The flanks of Bowie Seamount have average slopes of between 10°–20°, with significant local variation (Figure 3). The northeast and southwest flanks of the main edifice are more rugged than the northwest and southeast sides, with local slopes ranging between 0° and 50°, resulting from the presence of steep-sided, flat-topped terrace features that are most likely solidified lava lobes or lava lakes. The northwest side is characterized by a series of narrow, relatively deep, linear gullies separated by wider ridges. The top of the relatively smooth southeast flank displays sharp embayments that appear to cut the summit plateau.

#### 4.1.2. Denson

[15] Denson Seamount (Figure 4a) lies approximately 145 km north of the Bowie-Hodgkins seamount complex, and is separated from it and Dickins Seamount to the northeast by the Mukluk Channel [*Stevenson and Embley*, 1987] (referred to as the Tsimshian Seachannel by *Smoot* [1985]). Radiometric dating of transitional basalts gave ages between 16.8–19.7 Ma [*Turner et al.*, 1980], meaning that Denson formed on young crust (<4 Ma at the time of seamount formation) well before this area passed over the Bowie hot spot. In plan view the bathymetry shows a broadly circular rugged base, sloping up to a steep-sided, flat-topped summit plateau. The slopes are highly irregular, with a lobate, step-bench morphology. The summit plateau is characterized by gentle slopes (<5°) that dip outward in all directions from the pear-shaped central peak. Concentric rings at different elevations on the central peak also give it a terraced appearance similar to those found in regions of coastal uplift [e.g., *Lajoie*, 1986]. However, these terrace levels are not at a common depth or tilt, as they would be if they were wave-cut and affected by postformation tilting (notice how isobaths are offset from terrace slopes of Figure 4b). Instead, these terraces are most likely a stack of thick lava flows with steep sides and flat tops. Close examination of the southern edges of these terraces show that they drape downward into a depression in the summit plateau, as lava flows would do, but wave-cut terraces would not.

**Table 1.** Shape, Size, and Age Parameters for Gulf of Alaska Seamounts[a]

| Seamount | Base Depth, m | Peak Depth, m | Peak Latitude | Peak Longitude | Base Area, km$^2$ | Base Circumference, km | Summit Area, km$^2$ | Summit Circumference, km | Summit Shape | Base Shape | Approximate Volume, km$^3$ | Min. Plateau Depth, m | Max. Plateau Depth, m | Seamount Age, Ma | Seafloor Age, Ma |
|---|---|---|---|---|---|---|---|---|---|---|---|---|---|---|---|
| Bowie | 2800 | 34 | 53° 17′ 58.9″N | 135° 39′ 02.5″W | 700 | 122 | 26 | 31 | NE-SW elongate | linear | 857 | 200 | 250 | ≤0.7 | 16–17 |
| Denson | 3100 | 946 | 54° 4′ 36.5″N | 137° 22′ 11.7″W | 902 | 114 | 109 | 40 | NW-SE oval | round | 806 | 950 | 1250 | 16.8–19.7 | 20 |
| Dickins | 3000 | 419 | 54° 31′ 56.5″N | 136° 31′ 51.0″W | 664 | 168 | 18 | 7 | ENE-WSW elongate | linear | 693 | - | - | 2–4 | 20 |
| Welker[b] | 3300 | 759 | 54° 54′ 14.1″N | 138° 11′ 2.3″W | 742 (+ 239) | 118 (+ 101) | 104 | 49 | N-S irreg. | irregular oval | 988 | 750 | 910 | 14.9 | 23–24 |
| Pratt | 3700 | 719 | 56° 13′ 36.9″N | 142° 36′ 25.7″W | 1822 | 209 | 229 | 63 | E-W oval | oval | 2309 | 730 | 900 | 18 | 30 |
| Giacomini | 3900 | 648 | 56° 29′ 23.2″N | 146° 21′ 33.1″W | 1127 | 132 | 74 | 35 | E-W oval | round | 1342 | 680 | 730 | 19.9–21 | 33–34 |
| Ely | 3900 | 2129 | 56° 21′ 27.1″N | 145° 45′ 8.6″W | 348 | 74 | 9 | 11 | round w/pit | round | 268 | 2200 | 2250 | ? | 32 |
| Cobb | 3000 | 34 | 46° 45′ 17.9″N | 130° 51′ 58.0″W | 1316 | 145 | 61 | 31 | E-W oval | round | 1304 | 120 | 260 | 3.3 | 3.8 |
| Warwick | 3400 | 489 | 48° 5′ 27.8″N | 132° 48′ 17.0″W | 1537 | 212 | 42 | 25 | E-W oval | round/linear | 1514 | 500 | 650 | 6.9 | 10 |
| Scott | 4000 | 1005 | 50° 25′ 24.8″N | 141° 29′ 54.8″W | 1256 | 149 | 19 | 17 | dissected round | irregular oval | 1508 | 1080 | 1150 | ? | 28–29 |
| Campbell | 3900 | 1029 | | | - | - | - | - | oval irregular | irregular round | - | 1100 | 1200 | ? | 30 |
| Murray | 3300 | 572 | 53° 43′ 52.2″N | 148° 31′ 26.5″W | 629 | 101 | 3 | 7 | irregular | round | 1003 | 600 | 700 | 27.6 | 32–34 |
| Patton | 3900 | 160 | 54° 35′ 27.0″N | 150° 26′ 38.2″W | 1926 | 217 | 24 | 25 | irregular | irregular | 4226 | 330 | 430 | 29.7 | 42 |
| Marchand | 4000 | 1665 | 54° 55′ 23.8″N | 151° 21′ 42.4″W | 320 | 73 | 2 | 7 | E-W elongate | irregular round | 272 | - | 1885? | 26 | 43–44 |

[a] Seafloor ages are from *Atwater and Severinghaus* [1989]. Seamount ages are from *Cousens et al.* [1999] (Bowie); *Dalrymple et al.* [1987] (Welker, Murray, Patton); *Desonie and Duncan* [1990] (Cobb, Warwick); R. Keller et al., manuscript in preparation, 2007 (Pratt, Marchand); and *Turner et al.* [1973, 1980] (Bowie, Denson, Dickins, Giacomini).
[b] Values in parentheses for Welker represent the small rock mass attached to the NW corner of the seamount.

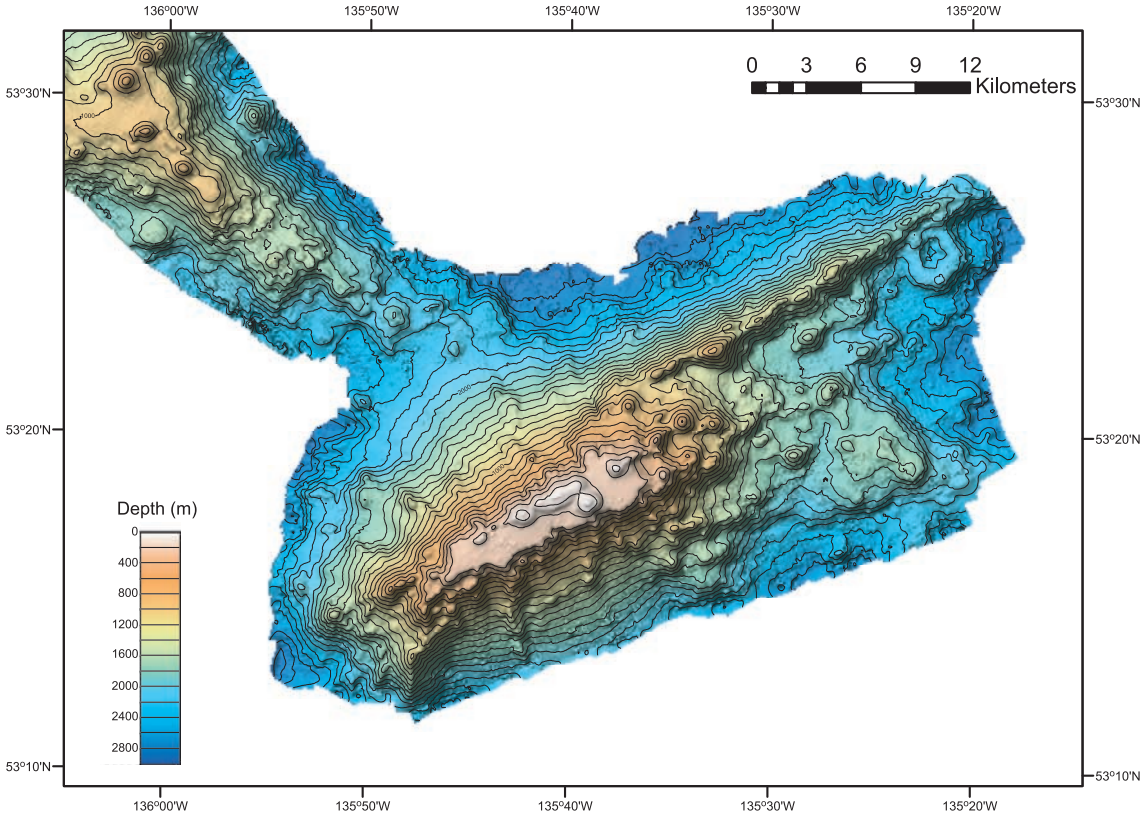


**Figure 3.** Color shaded-relief bathymetric map of Bowie Seamount. Data covering this seamount were collected by the NOS [*Herlihy*, 2000]. The contour interval is 100 m.

[16] The rugged bathymetry on the lower half of the seamount is composed of small flat-topped, sometimes cratered, circular volcanic cones and terraces that may represent tube-fed lava deltas similar to those found on submarine ridges in the Hawaiian Islands [e.g., *D. K. Smith et al.*, 2002]. Individual examples of these features vary in size up to a maximum diameter of ~2000 m and relief of over 200 m. The maximum measured depth of craters on those features is ~10 m from rim to crater bottom.

[17] The northern flank of the seamount is smoother and does not extend as far from the summit plateau. It appears that it is being undermined by erosion on the outside of a bend in the Mukluk Channel where the channel passes between Denson and Dickins seamounts (Figure 4), thus inducing flank collapse of this side of the seamount, although no debris field related to slope failures can be clearly identified. On the eastern flank of the seamount several linear scarp features cut from near the base toward the summit and form an approximate V-shaped embayment that may also represent evidence of incipient or previous slope failure.

### 4.1.3. Dickins

[18] While located less than 60 km from the summit of Denson Seamount, the morphology of Dickins Seamount is profoundly different in overall shape and slope characteristics (Figure 5). Like Denson, Dickins sits atop ~20 Ma crust of chron 6, but Dickins is much younger than Denson. According to K-Ar dating by *Turner et al.* [1980], Dickins is about 2–4 Myr old, which is approximately the right age for it to have formed at the Bowie hot spot.

[19] Dickins is dominantly a ~35 km long, ~20 km wide semi-linear, steep-sided edifice, but with associated linear ridges extending out from the southwest and northwest sections of the main seamount. The ~25 km long ridge extending off the southwest flank of Dickins may be from lateral flow of magma along a now buried fault or rift zone. The ridge to the northwest (Spur ridge of *Smoot* [1985]) is separated from Dickins by the

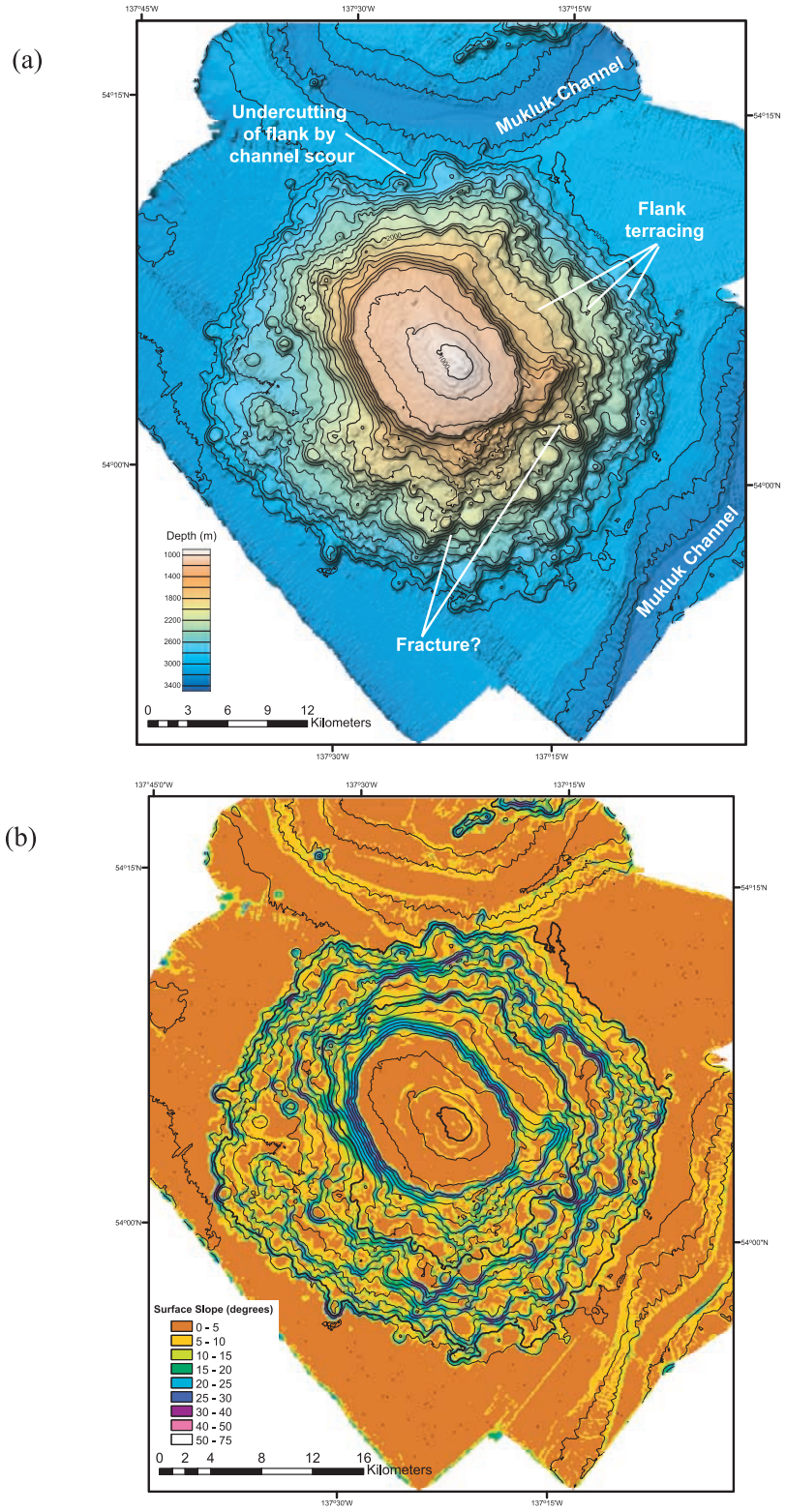


**Figure 4.** (a) Color shaded-relief bathymetric map of Denson Seamount, showing step-bench morphology resulting from repeated lava terrace construction and extensive development of small cratered and flat-topped volcanic cones on the lower flanks. The location of slope undercutting resulting from migration of the Mukluk channel, and possible incipient fracture scarps on the eastern flank are also indicated. Contour interval is 100 m. (b) Slope map of Denson Seamount derived from the bathymetry in Figure 4a showing the step-bench, lava terrace morphology characteristic of this and other seamounts in the Gulf of Alaska.

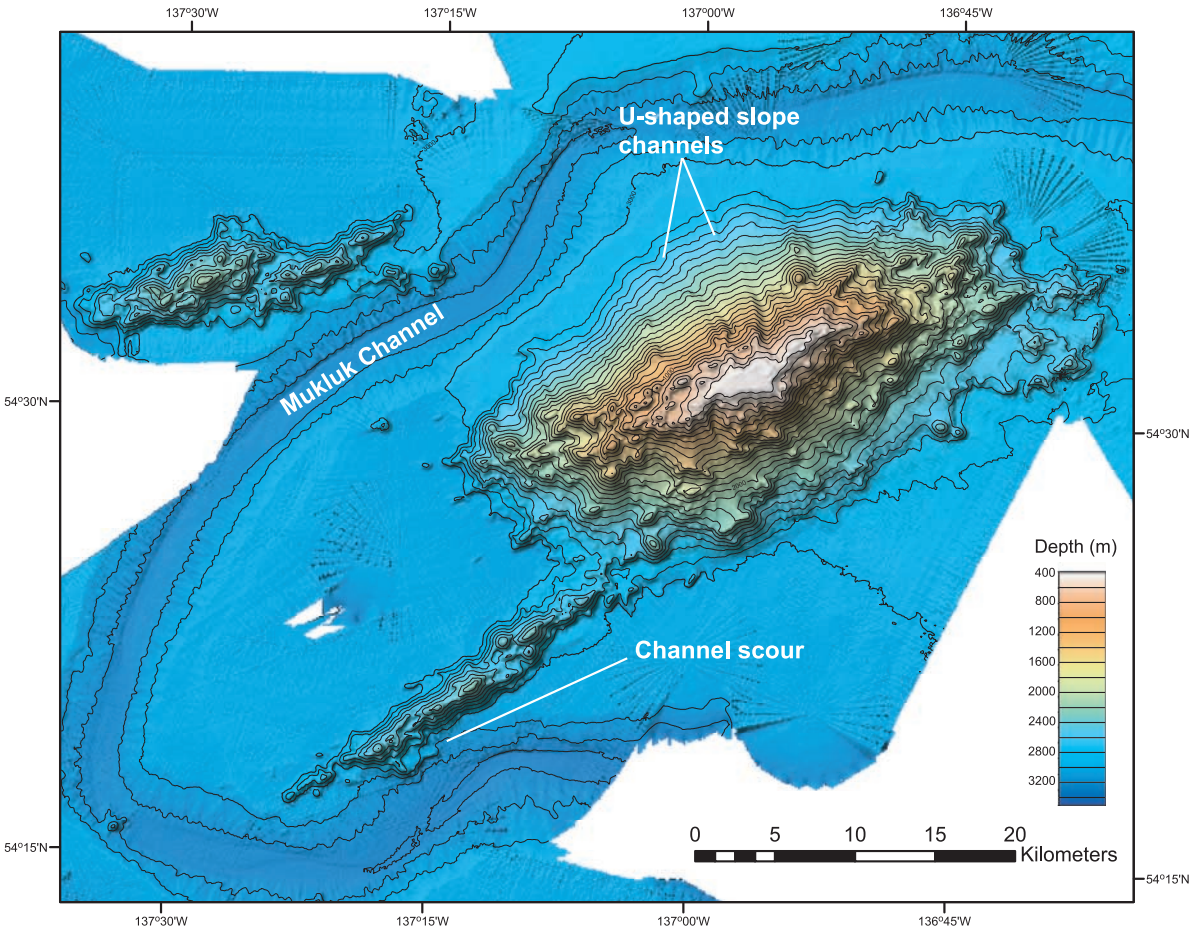


**Figure 5.** Color shaded-relief bathymetric map of the linear, ridge-like Dickins Seamount, adjacent spur ridges, and Mukluk Channel. Locations of possible slope failure-related u-shaped channels and channel scour of the southwestern spur ridge are indicated. The contour interval is 100 m.

Mukluk Channel, and appears to be a separate edifice, but may in fact prove to be temporally or spatially related. The summit plateau of Dickins is narrow, flat (average slope of <1°) and has a slight dip toward the south and southeast.

[20] The flanks of the seamount slope mainly between 10°–20° (Figure 5), with the highest slopes in general found on the northwest and southeast flanks, where local slope values exceed 30° in places. Like Bowie, the steep but narrow linear nature of the seamount has resulted in the northwest and southeast flanks displaying a smoother, somewhat fluted morphology with the northeast and southwest ends characterized by steep, closely spaced NE-SW trending linear ridges. Unlike the seamounts already described, lobate, flat-topped lava terraces are not present on the flanks of Dickins, suggestive of a different eruptive pattern or tectonic association.

[21] Although surrounded on three sides by the Mukluk Channel, the bathymetry reveals no evidence to suggest that the channel has yet begun to influence the morphology of the seamount in any significant way. The flow within the Mukluk Channel has begun to undermine the slopes on the ridge extending to the southwest of Dickins and also part of the southern side of the separate spur ridge. It does appear that the presence of the seamount has altered and constricted the path of the Mukluk Channel.

### 4.1.4. Welker

[22] As with Dickins Seamount, the age and position of Welker are consistent with it having formed at the Bowie hot spot. In plan view (Figure 6a), the base of Welker is almost rectangular, longer in the north-south direction at ~35 km than the east-west direction, which is ~25 km at the widest point. The

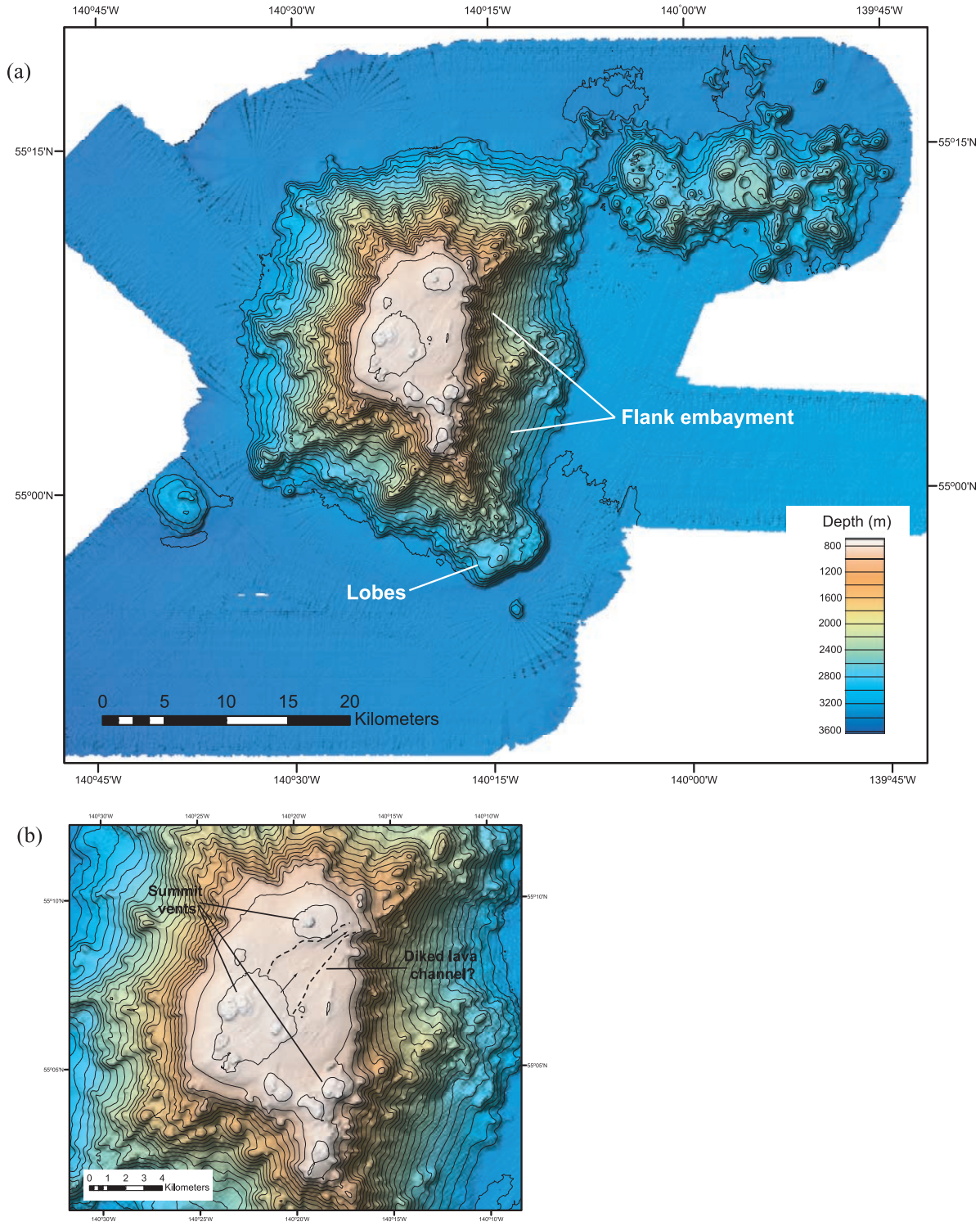


**Figure 6.** (a) Color shaded-relief bathymetric map of Welker Seamount. The locations of the lava lobes and possible slope failures discussed in the text are shown. Contour interval is 100 m. (b) Detail of the summit plateau of Welker, showing the location of volcanic vents and possible lava flow channel (indicated by dashed lines). Arrows indicate the potential direction of lava flow following eruption from the vents. Contour interval is 100 m.

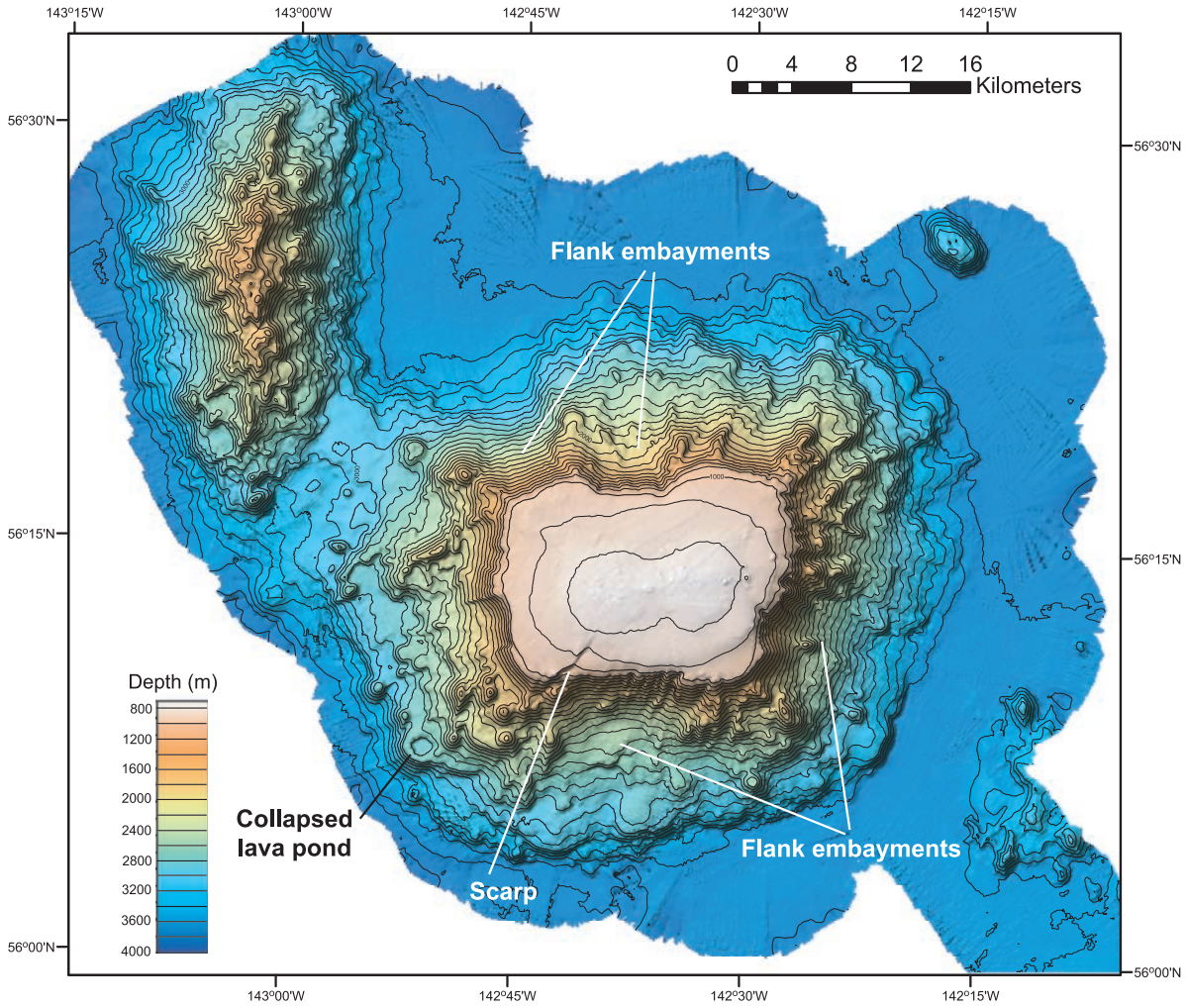


**Figure 7.** Color shaded-relief bathymetric map of Pratt Seamount and adjacent linear ridge. The strongly embayed nature of the summit plateau and flanks of the seamount, plus the presence of an incipient or abandoned headwall scarp cutting the summit, is suggestive of significant modification of the seamount via slope failures. Note the collapsed or incompletely filled lava pond on the SW flank. Contour interval is 100 m.

summit plateau of the seamount is overall relatively flat (mostly <1° slopes), but grades from smooth, flat plateau edges to irregular, high-relief pinnacles and channels (Figure 6b; discussed below). The flanks of the seamount have averaged slope values that range between 10° and 20°, with local slopes exceeding 30°, especially along the sides of the prominent radial ridges (Figure 6a).

[23] A significant spur ridge extends off the northeast flank, containing several circular, to semi-circular volcanoes with central and summit plateau-edge craters, similar in morphology to the volcanoes of the President Jackson and Taney Seamounts [*Clague et al.*, 2000b]. Visually, these features appear related to the larger edifice. Several smaller isolated volcanoes with summit craters are also visible on the abyssal plain surrounding Welker, partially covered by sediments.

[24] Although small, Welker displays some of the most compelling evidence of the volcanic constructional, rather than erosional, processes responsible for the evolution of these features. Close examination of the summit plateau (Figure 6b) reveals the presence of several broad domes capped by at least seven 30–50 m high volcanic cones, most of which are clustered in the southeast and southwest corners of the plateau. Closely linked to these cones is what appear to be a system of leveed lava channels (Figure 6b) that lead from some of the summit cones, across the summit plateau, and over

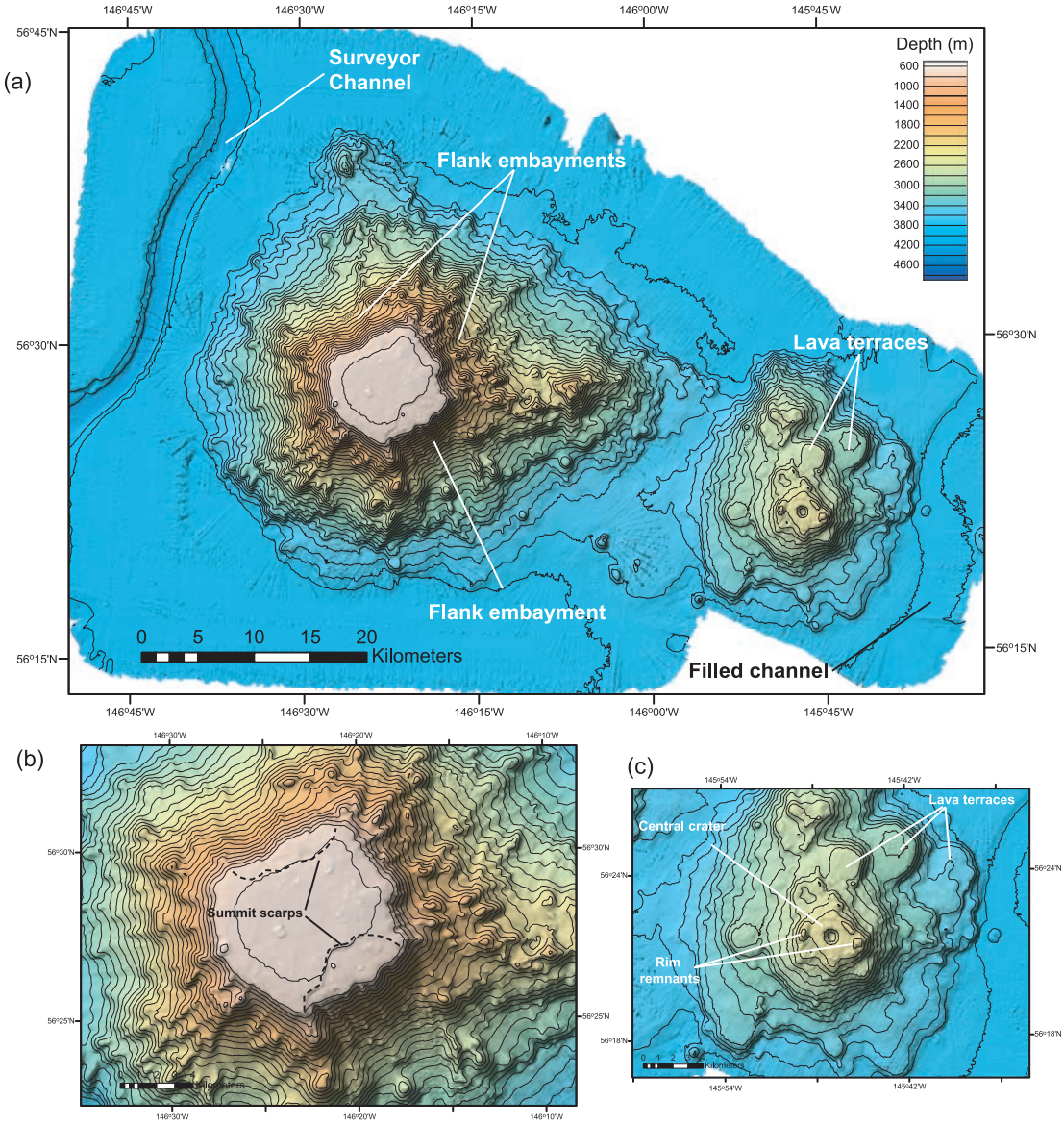


**Figure 8.** (a) Color shaded-relief bathymetric map of Giacomini (left) and Ely (right) Seamounts. The Surveyor Channel is seen to the west of Giacomini, with a subdued, unnamed channel to the east of Ely. (b) Bathymetry map of the Giacomini summit plateau, showing the locations of possible slope-failure related headwall scarps (indicated by dashed lines) above the northern and southern seamount slopes. Contour interval is 100 m. (c) Bathymetry map of Ely's summit, showing the small pit crater and remnants of the rim/levee that surrounded it. Contour interval is 100 m.

its northeast edge to be distributed down the flanks of the seamount via a series of slope channels.

### 4.1.5. Pratt

[25] Pratt Seamount lies ~190 km (summit-to-summit distance) northwest of Welker, separated from it by the flat-topped Durgin Seamount (Figure 1). An unnamed linear ridge intriguingly similar to Dickins Seamount in overall shape extends off the northwest corner of the main edifice (Figure 7). This ridge may be the result of a prolonged flank eruption or an early phase of Pratt's formation. Separating the two features is a low bathymetric saddle, a portion of which has clearly visible semi-circular to circular depressions that resemble collapse pits on an underlying lava conduit or partially filled volcanic cones.

[26] Although the summit plateau is overall relatively flat (average slope <1°), a broad dome with as much as 100 m of relief is present over the central part of the plateau. In addition, several small hills occur at the center and eastern edge of

the summit plateau. The summit plateau is rimmed on all sides by steep, linear to curvi-linear scarps with slopes that exceed 40° in places (Figure 7). Below these, the slopes progressively decrease down to as low as 10°–20°, in most cases via a series of tilted lobate lava terraces. A lava terrace topped by a well-expressed circular or ring-shaped levee with a diameter of ~1 km and a height of ~100 m is visible on the southwest flank of the seamount. This feature appears to be the collapse of an early phase of lava pond formation before the central crater (pond) was filled, and is similar to examples found on the subaerial [*Wilson and Parfitt*, 1993] and submarine [*Clague et al.*, 2000a] parts of the active Hawaiian Island volcanoes.

[27] Embayments in the edges of the summit plateau along with oversteepened scarps and smooth, chute-like features separated by ridges, suggest that the flanks of Pratt have undergone significant modification by slope failure. A ~7 km long scarp can be seen cutting into the southwest corner of the summit plateau and upper flank of the seamount (Figure 7). Vertical separation across the scarp increases from zero at its northeast end, to more than 100 m at the edge of the summit plateau. This feature may be the headwall scarp of an incipient or failed slope failure.

### 4.1.6. Giacomini and Ely

[28] Giacomini Seamount (Figure 8), another large, flat-topped seamount, is the tallest and next-to-oldest of the seamounts in the Kodiak-Bowie chain. It rises 3300 m above the regional seafloor, and yielded K-Ar ages between 19.9 Ma and 21 Ma [*Turner et al.*, 1973, 1980]. In plan view, the base of Giacomini is circular to elliptical, but pointed on its eastern side resulting from lateral volcanic construction. The 700 m deep summit plateau has an average slope of less than 1°, although numerous small mounds that are less than 100 m high, are present. To the west of Giacomini lies the Surveyor channel [*Ness and Kulm*, 1973], which has thalweg depths in excess of 250 m as it passes Giacomini, separating Giacomini from Kodiak seamount and the Aleutian trench.

[29] The flanks of Giacomini have overall average slopes of between 10°–20°, being steeper on the upper parts of the flanks (20°–30°), decreasing to 10°–15° near the base. In general, the flanks of Giacomini are dominated by irregularly shaped ridges, with small pointed volcanic cones and lava terraces present on the lower slopes. The basal morphology is less sharp than that seen on other seamounts in the region, which may be the result of extensive sedimentation around the base. On the southern edge of the summit plateau, a 20 m high curved scarp is visible above one of the few predominantly smooth slopes on the flanks of the seamount (Figure 8b). As with the scarp on Pratt, this feature may be the headwall scarp of an incipient or abandoned slope failure, in an area of the seamount that bears morphology suggestive of previous failures. A similar, but more subdued headwall scarp may be present on the northwest edge of the summit plateau, just above another relatively smooth area of the seamount flank, suggesting that significant failures may have occurred on this side of the seamount also.

[30] Although small, Ely Seamount is mentioned here because it exhibits the flat top and terraced flanks of many of the others, but is unique among the seamounts in that its summit plateau is ringed by a levee (or a caldera rim?) and has a pronounced crater in its center. The base and flanks of Ely are dominated by the extensive development of flat-topped lava terraces. The summit plateau has a diameter of approximately 4 km with 100 m high rim levees and a 200 m deep crater (Figure 8c). A thick sequence of well-layered sediments, imaged by 3.5 kHz subbottom profiling, has accumulated within the crater. The restricted depositional environment and thickness as imaged, suggest that this accumulation is composed almost entirely of pelagic/hemipelegic, with minor deposits of crater wall material. A subdued sea-channel immediately east of Ely, separates it from Quinn Seamount.

## 4.2. Cobb Seamount Chain

### 4.2.1. Cobb Seamount

[31] Cobb Seamount is just 100 km to the west of the currently active location of the Cobb hot spot at Axial Seamount on the Juan de Fuca Ridge (Figure 1). A single radiometric age of ~3.3 Ma [*Desonie and Duncan*, 1990] is only ~0.5 m.y. younger than the age of the underlying crust (Chron 2A [*Atwater and Severinghaus*, 1989]).

[32] Rising from a broadly circular rugged base at ~3000 m, the flanks of Cobb are characterized by a lobate, step-bench morphology sloping up to a steep-sided, flat-topped summit plateau at a depth between 200 and 300 m (Figure 9). The summit plateau is characterized by gentle slopes (<3°) that dip outward in all directions via a series of weakly defined steps. Several raised peaks are seen within the central part of the plateau, reaching a minimum

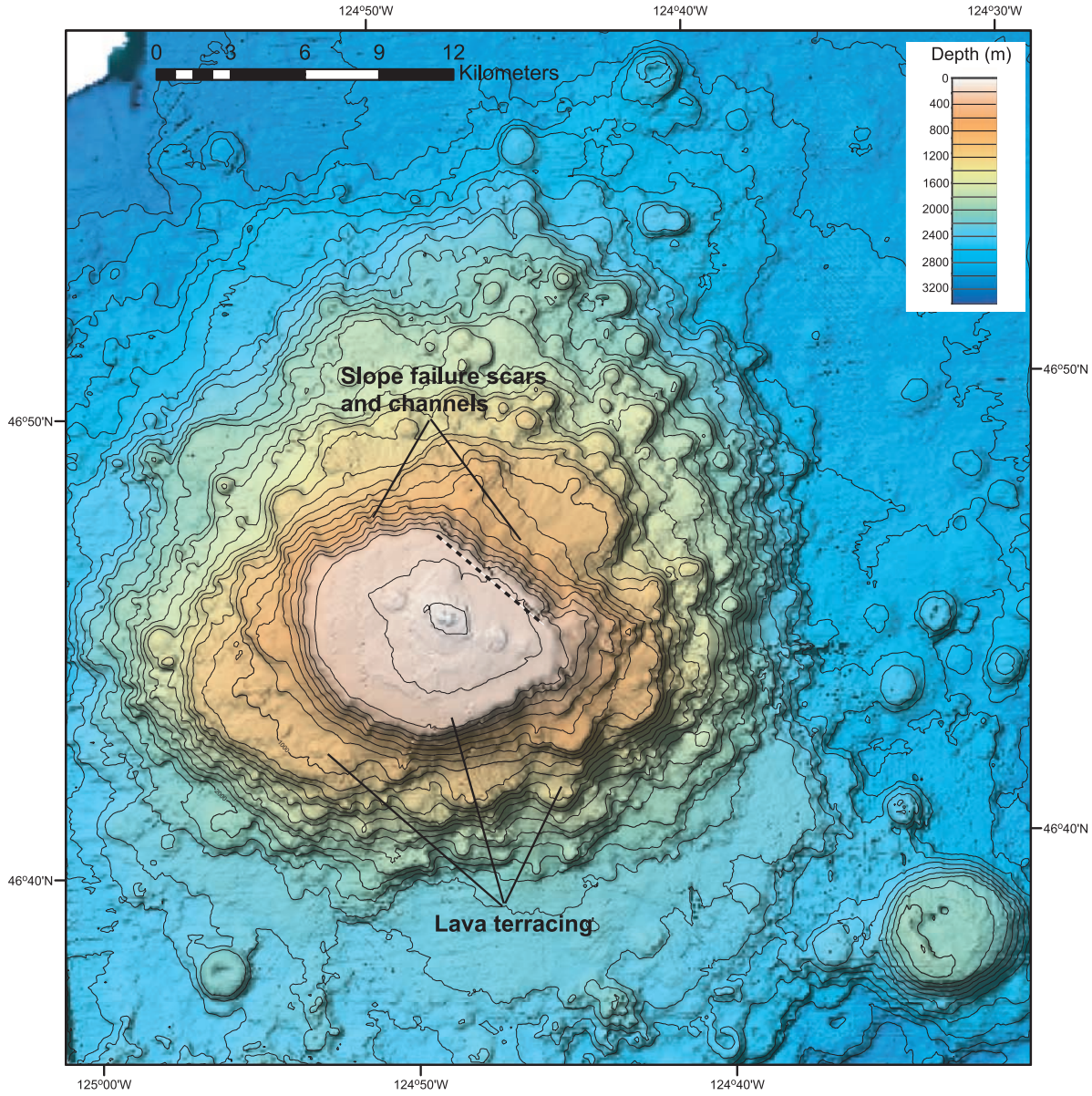


**Figure 9.** Color shaded-relief bathymetric map of Cobb Seamount showing the well-developed step-bench, lava terrace, and crated cone morphology. The locations of significant slope failures and slope channels are indicated. The dashed line indicates the location of summit flank shape modification by slope failure processes. Contour interval is 100 m.

depth of 34 m. Well-developed, flat-topped lava terraces and cones cover the flanks of the seamount. Although the average slopes of the flanks are less than 15°, slopes commonly exceed 30° around the edges of lava terraces, increasing to over 45° in places (Figure 9). In addition to the larger terraces, numerous smaller discrete circular, flat-topped, rounded, or crated volcanic cones are present, largely restricted to the lower sections of the seamount's flanks. Southeast of the main seamount edifice is a single large volcanic cone over 5 km in diameter and up to 1000 m tall, with a relatively shallow pit crater at its summit and a bulbous overall shape. This cone could be related directly to Cobb or to a younger eruptive phase such as the Brown Bear Seamount closer to the ridge.

[33] Well-pronounced embayment and linearization of the edge of the summit plateau is seen on both the northeastern and northwestern sides of the seamount (Figure 9), with a somewhat more weakly defined embayment of the western side. *Bobbitt et*

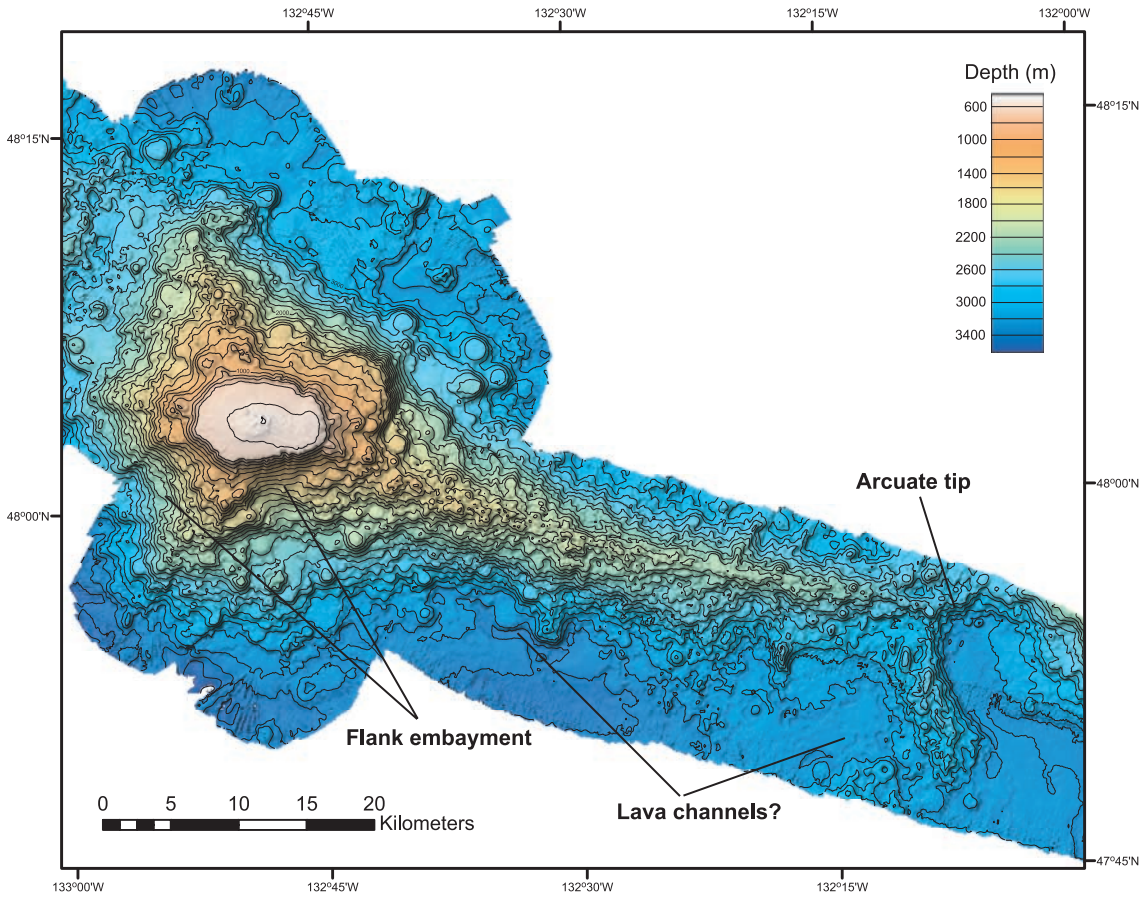


**Figure 10.** Color shaded-relief bathymetric map of Warwick Seamount. The morphology of Warwick is composed of the main flat-topped edifice, with a linear ridge extending from it toward the SE and flanks dominated by lava terraces. The locations of flank embayments and what are possibly collapsed or abandoned lava channels are shown. Contour interval is 100 m.

*al.* [2000] attributed the smooth morphology of the slope section directly below the northeast edge of the plateau to flank failures. Channels cut into these slope failure scars may have formed during repeated debris flows during the period when the summit of Cobb was near sea level. In marked contrast to other seamounts in the Gulf of Alaska, there is evidence that the summit plateau of Cobb was above sea level. Submersible dives located wave-cut terraces at 82 m and 219 m deep [*Schwartz*, 1972; *Schwartz and Lingbloom*, 1973], and rounded beach cobbles and intertidal mussel shells at 115–150 m deep [*Budinger*, 1967]. Some of these terraces have slope angles and outlines that differ and are more varied than the volcanically created terraces on other seamounts in the Gulf of Alaska. For example, the eastern edge of the 85-m deep terrace (marked by a dashed line in Figure 9), is nearly straight in a NW-SE direction and has a steeper slope than the other faces of that terrace, suggestive of posteruptive slope modification.

### 4.2.2. Warwick

[34] Warwick Seamount has a composite morphology, comprising a circular to semi-circular main edifice and a tapering topographic ridge to its southeast (Figure 10a). The seamount extends ~70 km in a northwest-southeast orientation, but only ~30 km in the northeast-southwest direction. An oval summit plateau, with a raised dome in the center, caps the main edifice. The top of the dome marks the summit of the seamount at a depth of 489 m. The local basal depth in this area is at 3300 m, giving Warwick vertical relief of approximately 2800 m.

[35] The summit plateau is surrounded on all sides by moderately steep slopes, which in places exceed 30° (Figure 10b), and embay the edges of the

plateau in several locations. The sharpness of the embayments at these summit edges, and the relatively smooth upper flanks of the seamount below them may be the result of slope failures. Apart from these areas of apparent slope failures, most of the flanks of the seamount are a series of lava terraces and small circular flat-topped and cratered cones. These cones occur in a wide range of sizes, some with diameters of over 2000 m, heights exceeding 200 m and where present, summit craters commonly 20 m or more deep. Many of the smaller flat-topped cones display a somewhat rugged morphology over part or all of their summits, mirroring to some degree the morphology of the summit plateau of the main edifice.

[36] The long straight ridge extending off the southeast side of Warwick, extends for over 45 km toward the Juan de Fuca Ridge (Figures 1 and 10) and is morphologically similar to rift zone-related ridges [e.g., *Lonsdale*, 1989; *D. K. Smith et al.*, 2002], perhaps in this case tracing a leaky transform. The surface morphology of the ridge is extremely rugged, with far fewer distinct lava terraces and cones than seen on and around the main edifice and other seamounts within the gulf. This morphology seems suggestive of eruptions of short duration or from a diffuse outlet. The arcuate tip of the ridge is similar to the tip of the Hana Ridge in Hawaii, which may be constructional or from collapse [*J. R. Smith et al.*, 2002; *Eakins and Robinson*, 2006].

[37] Another interesting morphologic feature seen only at Warwick, are small, curved, flat-bottomed "channels" at the base of the seamount (Figure 10). These channels are up to a few hundred meters wide and tens of meters deep. Some of them completely surround small volcanic cones or simply follow the base of the seamount, while others show no preferred orientation or controlling morphology. They may be collapse features in sheet flows on the surrounding seafloor, but it is unclear why the sheet flows would preferentially collapse around preexisting features.

### 4.2.3. Scott

[38] Scott Seamount, along with Campbell, T. Horton, Pathfinder seamounts and several smaller unnamed features, is located within the central Gulf of Alaska, over 680 km northwest of Warwick (Figure 1). Scott sits on 28–29 Ma crust between chrons 9 and 10 [*Atwater and Severinghaus*, 1989], but no radiometric age has been determined for Scott. It is assumed to be slightly younger than the ages of 23.1 Ma [*Dalrymple et al.*, 1987] and 20.7 Ma [*Turner et al.*, 1980] for the nearby Pathfinder and T. Horton seamounts, respectively. *Dalrymple et al.* [1987] puts Scott (as well as T. Horton and Pathfinder) in a seamount chain separate from and south of the Cobb chain, but the plate motion models of *Wessel et al.* [2006] put Scott on the Cobb hot spot track. *Turner et al.* [1980] also attributes T. Horton (and thus presumably the nearby Scott) to the Cobb hot spot.

[39] Scott is a large and chaotic volcanic body (Figure 11), elongated in the northwest-southeast direction, with the primary summit plateau located at the northwest end and a secondary plateau near the southeast end. The summit peak depth of 1005 m is found on a raised section of the primary summit plateau. The east and south flanks of the primary summit plateau are extensively incised by channels, possibly the result of constructive volcanic processes (e.g., leveed lava channels), post-eruptive slope modification, or a combination of processes. Similar flank morphology and summit embayment can be seen around the secondary plateau.

[40] Much of the edifice, especially away from the primary summit plateau is composed of circular cratered and flat-topped, steep-sided lava terraces of various sizes (Figure 11b). The construction of Scott appears to be the result of a continuous process of lava pond filling and overtopping and subsequent solidification. Steep, irregular ridges are found on the highest parts of the seamount flanking the primary and secondary peaks. Like other seamounts in the Gulf of Alaska, the average slope of the flanks of Scott are between 10° and 20°, but locally exceed 30°, most notably around lava terraces and the primary summit plateau (Figure 11). A single transit swath across Campbell Seamount, ~30 km west southwest of Scott (Figure 11), reveals that it is similar in form to the primary edifice at Scott.

### 4.2.4. Murray

[41] Murray Seamount is at the eastern end of the Patton-Murray seamount platform, approximately 620 km northwest of Scott Seamount (Figure 1). In plan view, Murray is pear-shaped, oblate in the southwest part and dominated by the conical main edifice, becoming more linear and diffuse in the northeast (Figure 12a). The summit of Murray is at a depth of 572 m on a small hill on the southeast corner of the somewhat dome-shaped summit plateau. Murray rises approximately 2700 m above its

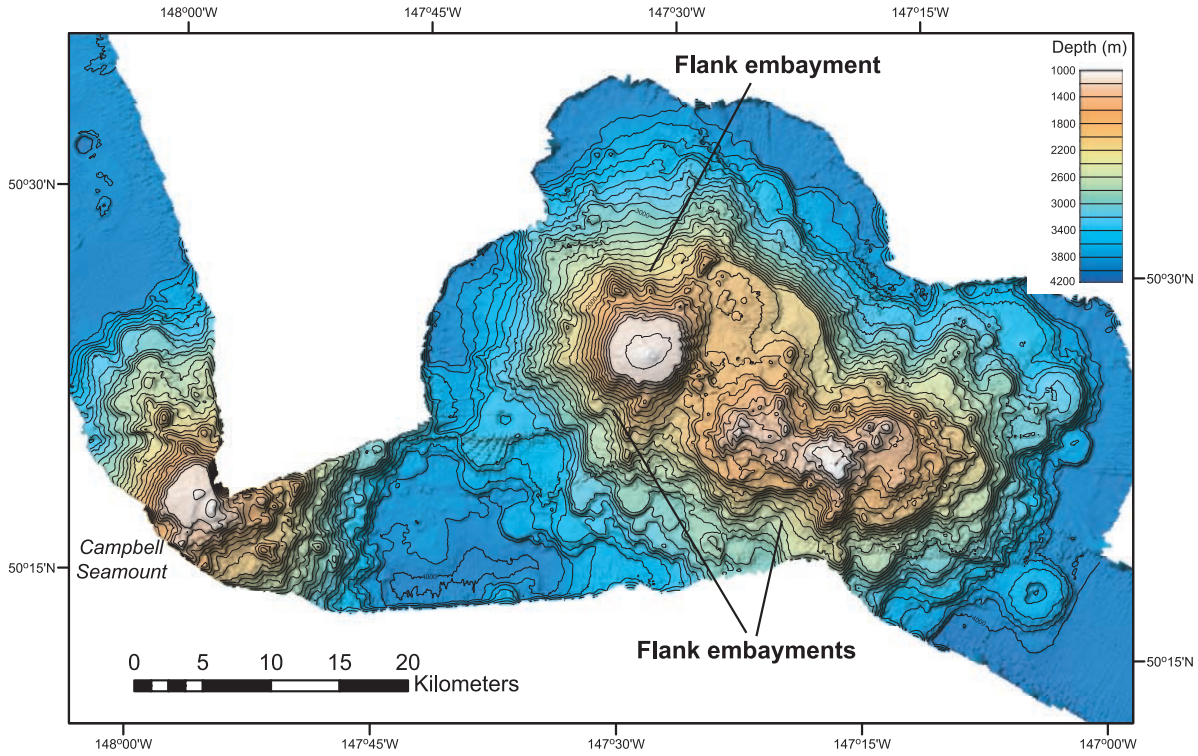


**Figure 11.** Color shaded-relief bathymetric map of Scott Seamount (with Campbell Seamount on the left). The morphology of Scott is dominated by numerous flights of overlapping lava terraces and cratered flat-topped volcanic cones. The primary flat-topped summit plateau of Scott is to the NW, with a more chaotically shaped secondary peak to the SE. The locations of possible slope failures are indicated. Contour interval is 100 m.

3300 m deep base at average slopes of between 10° and 20° (Figure 12b; except along the northeast flank). Slope values increase toward the summit, commonly changing to between 20° and 30° surrounding the summit plateau, but exceeding 45° in places.

[42] The upper flanks of Murray are dominated by linear volcanic ridges that radiate outward from the summit plateau which in turn separate regions where the flanks have a significantly smoother, chute-like morphology. At the bases of these chute features, the morphology is relatively subdued, blurring the transition from seamount to regional abyssal plain, although some flat-topped volcanic cones are still visible on the lower slopes. This morphology may be the result of extensive flank modification by slope failures. The relatively small summit plateau on Murray, when compared to those on much younger seamounts in the Gulf of Alaska, supports such an interpretation. The broad ridge on the northeast flank of Murray still contains well-preserved examples of flat-topped lava terraces and cones.

### 4.2.5. Patton

[43] Patton Seamount is located at the western end of the Patton-Murray seamount platform (Figure 1) [*Keller et al.*, 1997] at the southern terminus of the Surveyor deep-sea fan system [*Stevenson and Embley*, 1987]. Patton is composed of the main seamount edifice, connected by a low saddle to a smaller secondary peak to the southeast (informally referred to here as Codman Seamount; Figure 13), and an even smaller cratered volcanic cone to its east. Patton's irregularly shaped summit plateau at ~350–400 m depth is complex, with the south end of it being generally shallower, even though the shallowest depths are on some pinnacles scattered on the northern end of the plateau. The basal depth for this seamount is approximately 3900 m, making it the tallest seamount in the Gulf at ~3740 m.

[44] In plan view (Figure 13), the main body of Patton is elongated in the north-south direction,

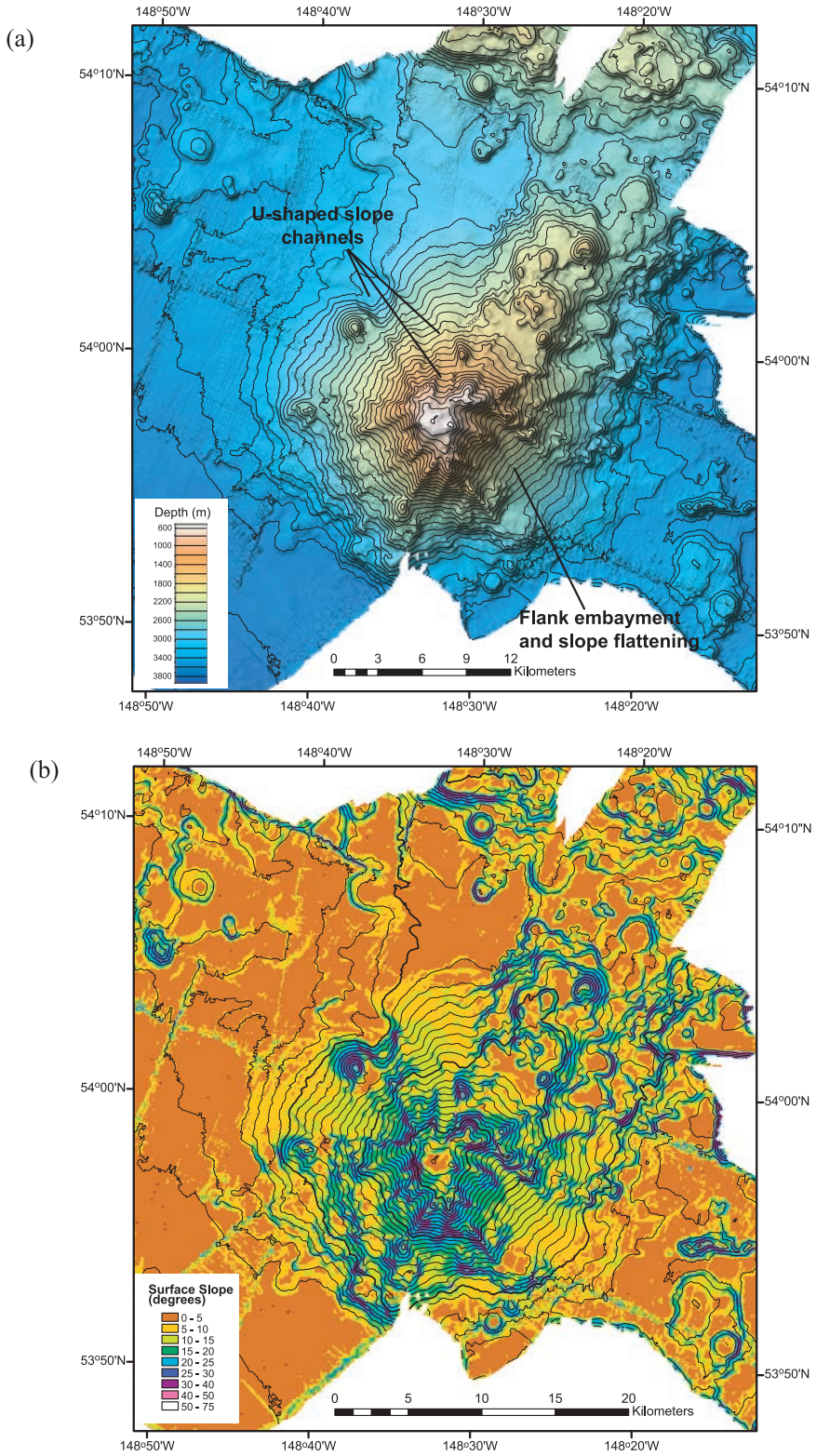


**Figure 12.** (a) Color shaded-relief bathymetric map of Murray Seamount. The locations of possible slope failures occurring below sites of summit embayment are indicated. Contour interval is 100 m. (b) Slope map of Murray Seamount derived from the bathymetry in Figure 12a, which, when compared to Figure 4b, shows the variation of flank and summit morphology of seamounts in the Gulf of Alaska.

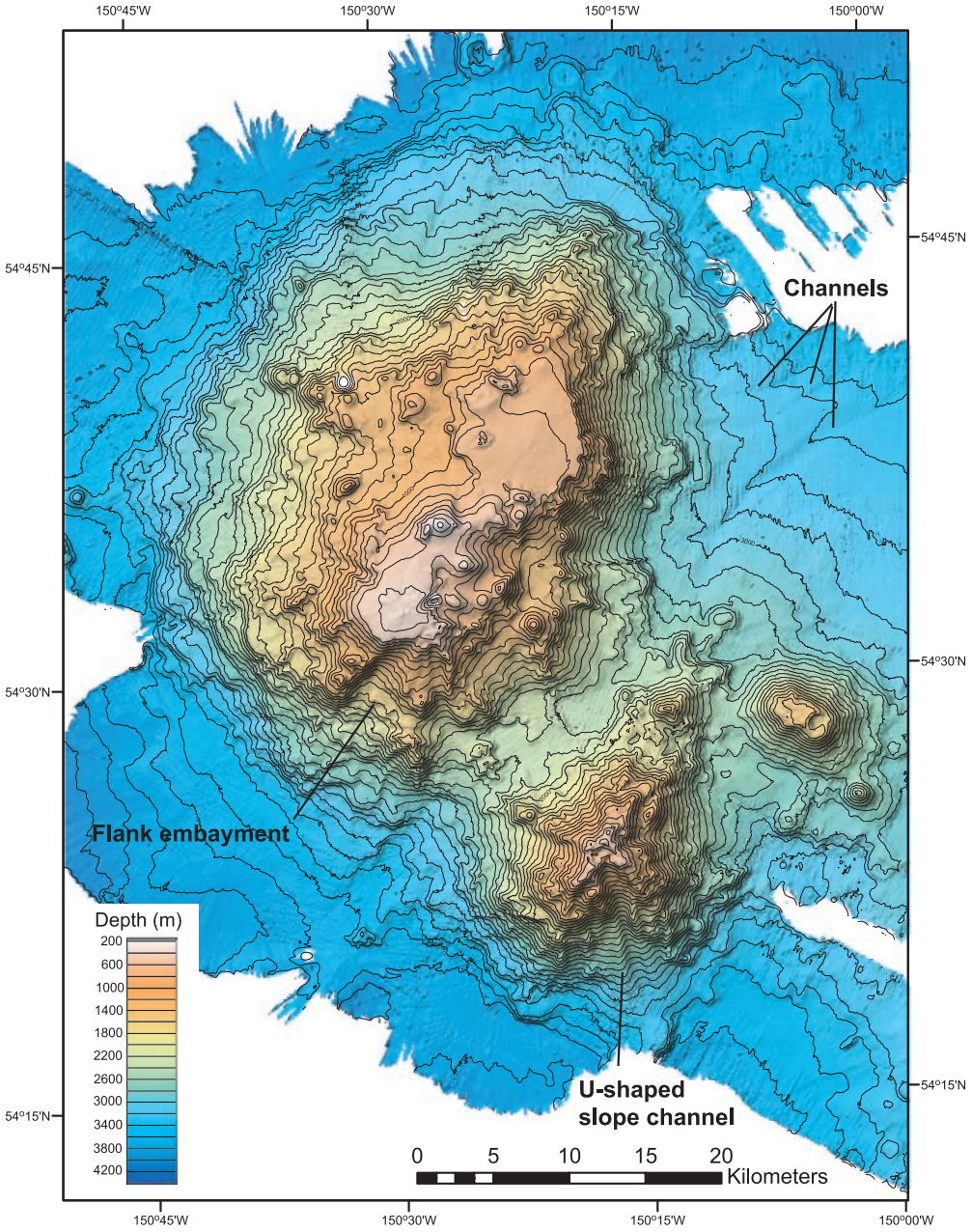


**Figure 13.** Color shaded-relief bathymetric map of Patton seamount complex, composed of Patton Seamount (the main edifice), Codman Seamount (the smaller, cone-shaped edifice south of Patton), and a smaller cratered volcanic cone, east of Codman. Note the development of channels on the abyssal plain originating from the NE flank of the seamount. Examples of flank embayment and u-shaped channels can be seen on both Patton and Codman Seamounts. Contour interval is 100 m.

giving it an elliptical basal outline. Although the overall morphology of the seamount is relatively smooth, several steep volcanic ridges, volcanic cones, and slope channels/chutes can be seen on the seamount flanks surrounding the primary summit plateau. Like other seamounts in the region, the flanks of Patton have average peak to base slopes of between 10° and 20° (Figure 13), except for the northern flank which displays a broad, relatively flat (<3°) bench at ~750 m depth. Steep, incised scarps embay the eastern edge of this bench, which may reflect flank modification by slope failures. Several clearly discernable channels originate on this eastern flank of the seamount and create a network of minor channels in the abyssal plain sediments below that flow downslope to the north-

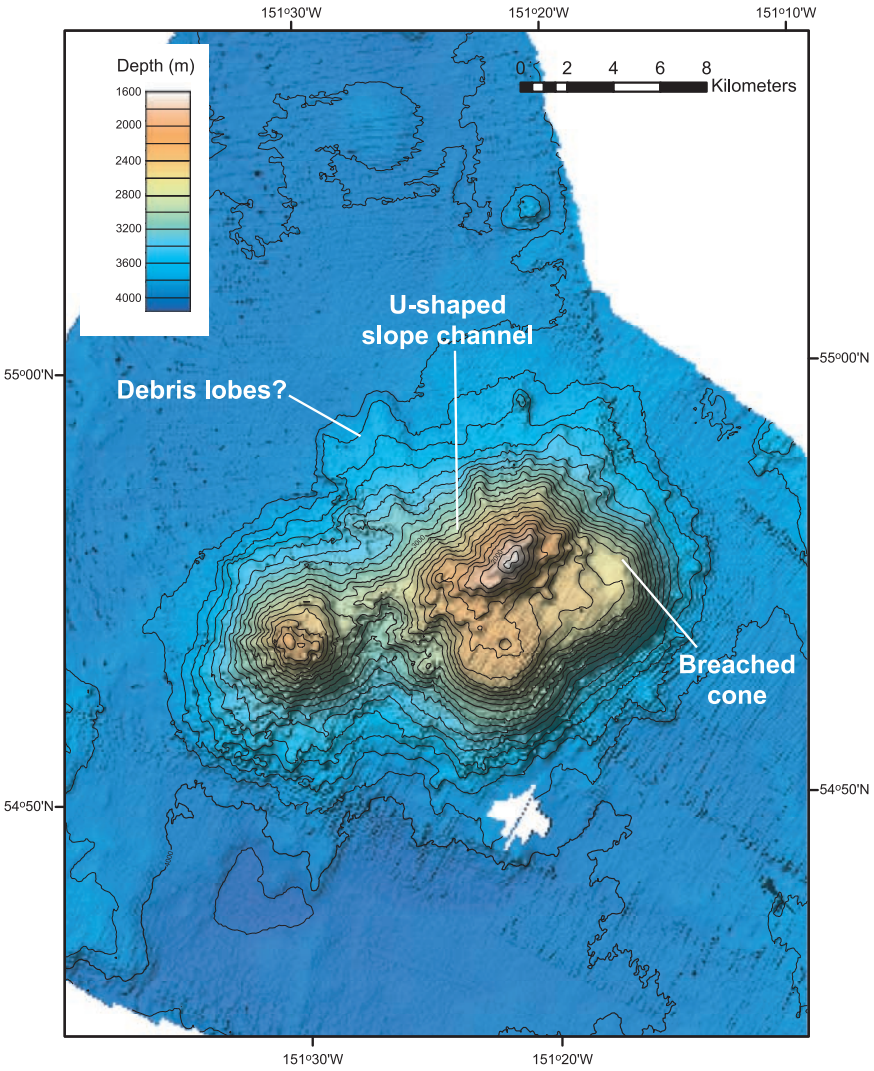


**Figure 14.** Color shaded-relief bathymetric map of Marchand Seamount, showing a broad bench composed of two cones, one with a centrally located crater and the other with a crater breached on its NE flank. Note the lack of distinct summit plateau at the shallowest depth on the seamount. Contour interval is 100 m.

east (Figure 13). Terracing and lobate flow-type morphology is present on the lower flanks of the seamount, but is subdued compared to most of the younger seamounts, probably due to slope failures and thick sediment deposition.

[45] Just southeast of Patton, Codman Seamount rises approximately 3250 m up slopes of between 10° and 20° (Figure 13b), to a summit depth of 450 m. The flanks of Codman are dominated by volcanic ridges and interridge chutes that radiate out from the seamount's small summit plateau. The summit of Codman appears to be the remnants of a breached caldera. The southern half of the caldera rim is missing, but in its place is a prominent u-shaped chute that leads down the southern flank to a bulbous lobe (debris pile?) at the foot of the seamount. Well-developed u-shaped chutes are also obvious on the northern and western flanks of Codman.

### 4.2.6. Marchand

[46] Marchand is the westernmost of the seamounts in the Cobb chain discussed in this study, located just southeast of the Aleutian trench. $^{40}$Ar-$^{39}$Ar dating of two rocks from Marchand yielded ages of ~26 Ma, similar to the ages of Murray and the youngest features dated on Patton (R. Keller et al., manuscript in preparation, 2007). In plan view (Figure 14) Marchand is elongated in the east-west direction (22 km E-W versus 15 km N-S), with two distinct peaks separated by a low bathymetric saddle. Unlike the majority of seamounts in the

Gulf of Alaska, Marchand lacks a distinct summit plateau at or near the shallowest depth of the seamount, although a broad bench at ~2300 m depth on the southeast flank of the seamount has the same subtle doming as some of the summit plateaus in this region, as well as a 50 m deep pit crater. This bench may have once been the summit plateau, but has since been topped by the tall peak on its northern margin. The flanks of Marchand are relatively smooth and featureless, and have average slopes of 15° to 20° (Figure 14), slightly higher than the average slopes of other seamounts in the gulf. The basal contact of the seamount is relatively subdued, in most cases merging with the abyssal plain without significant slope inflection. While the western peak is morphologically simple, forming an overall conical shape, the summit edifice of the eastern peak displays minor ridges that radiate away from the summit. The westernmost of these circular features is relatively complete, with a centrally located crater, while the crater on the northeast structures appears to be breached, either during its formation, or due to subsequent crater wall failure, creating an amphitheater-like morphology.

## 5. Discussion

[47] In general the overall shape of each of these seamounts is the result of original and evolutionary volcanic processes, slope failures, and hemipelagic and submarine fan sedimentary deposition. These new data allow us to explore the possible causes of some of these morphologic features, although a more thorough understanding will only come from additional investigation of these seamounts.

### 5.1. Flat-Topped Seamounts

[48] A number of mechanisms have been proposed to explain the presence of flat summit plateaus on seamounts, with many comparisons made to subaerial volcanic processes occurring on Hawaii and the Galapagos Islands. Strong evidence has been found for processes such as eruptions from circumferential feeders [e.g., *Batiza and Vanko*, 1984; *Fornari et al.*, 1988], erosion at the sea surface and subsequent large-scale subsidence [e.g., *Turner et al.*, 1980; *Detrick and Crough*, 1978], infilling of early stage summit calderas by renewed eruption and lava ponding [*Clague et al.*, 2000b], and cone sheets [*Mitchell*, 2003].

[49] Clear examples of partially and completely constructed flat-topped lava cones and terraces are seen on the flanks of almost all the seamounts described in this study. Lava ponding and inflation inside levee ringed summit areas would also explain the nearly horizontal summit plateaus on these seamounts. Almost all of the summit plateaus show evidence of a raised central section or scattered circular features similar in appearance to small volcanic cones. These may be late-stage volcanic features that formed on top of the solidified lava ponds. *Clague et al.* [2000a] determined a number of conditions required for the eruptive formation of flat-topped volcanic cones, including low- to moderate-rate effusion, eruption from a point source over long time periods, low slopes, and low viscosity basaltic lavas. These conditions appear to apply equally well to seamounts of all sizes in the Gulf of Alaska. All of the seamounts, except possibly Marchand, have flat tops, suggesting long-lived point sources of lava. Mildly productive hot spots such as Bowie and Cobb would provide the necessary conditions set forth by Clague et al.. In most cases, the extensive stacked sequence of solidified lava cones and terraces on the flanks of these seamounts suggest that each spent a significant amount of time as the outlet for the hot spot lavas. Subsequent late-stage or rejuvenated volcanism may have occurred after transport away from the hot spot source, creating the small cones and mounds on some of the summit plateaus. Marchand's apparent lack of a summit plateau may be deceptive. What appears to be a broad bench next to the summit peak may be the remnants of the former summit plateau, with the peak being an unusually large summit cone that obscures the rest of the former summit plateau. Since Denson is too old to have formed over the Bowie hot spot, unusually robust near-ridge melting anomalies may also provide the necessary conditions for creating a flat top [*Clague et al.*, 2000b].

[50] *Turner et al.* [1980] proposed a period of wave erosion followed by subsidence to explain the prevalence of flat-topped seamounts in the Pratt-Welker chain. Their model used the coupled hot spot subsidence mechanism proposed by *Detrick and Crough* [1978] and *Crough* [1978] for Pacific seamount chains, in which passage of lithosphere over a hot spot causes reheating and shallowing of the seafloor placing the summit regions at or above sea level. Continued plate movement and the subsequent lithospheric cooling and contraction result in the subsidence of the entire edifice to increasing depth with time. There are places in the ocean where this model clearly applies (e.g., Hawaiian and Cook-Austral chains [*Crough*,

1978; *Detrick and Crough*, 1978]), but not in the Gulf of Alaska. A total of 29 submersible dives on Gulf of Alaska seamounts (except for Cobb Seamount) found no evidence for wave erosion such as wave-cut terraces or cobble/sand beaches such as those seen on seamounts of the coast of California [e.g., *Paduan et al.*, 2004]. While it may be reasonable to assume that the pinnacles that extend to within 50–150 m of the sea surface on Patton and Bowie, and the terraces on the summit plateau of Cobb Seamount are all shallow enough to be within the range of past sea level drops, the flat summit plateaus found at 235 m (Bowie) to 2225 m deep (Ely) apparently were not. On the basis of the widespread occurrences of flat-topped cones and lava terraces at a variety of depths, these flat-topped seamounts can be constructed in this way entirely by volcanic processes. Even the concentric rings around some of the summit cones (especially Denson and Scott) are volcanically created lava terraces. Each of the terrace levels visible on these seamounts is too radially symmetrical to have been created by wave erosion.

[51] Ely Seamount (on Figure 8 with Giacomini) is an excellent illustration of the volcanic processes that work to create a flat-topped seamount. With a summit plateau at over 2200 m depth, this seamount was never above sea level. The floor of the crater in the middle of the summit plateau is 200 m deeper than the surrounding plateau, and looks exactly like pit craters formed by collapse of the upper crust of a lava pond after the lava drains away [*Clague et al.*, 2000b]. Subtler versions of collapse pits are also found on some of the lava cones and terraces on many of the other Gulf of Alaska seamounts. The summit plateau on Ely is nearly surrounded by a 20–100 m tall ridge that appears to be the remnants of a caldera rim. The plateau-forming lava pond that partly drained to allow the central pit crater to collapse must have mostly filled a preexisting caldera. If Ely had continued to build, it would have eventually completely refilled this caldera, creating a flat to gently domed summit plateau. As conduits feed lava from below it forms an upper crust that then grows upward through inflation, and outward by repeated overflows and self-repairs of the surrounding lava levees [*Clague et al.*, 2000b]. Each overflow occurs at the low point of the surrounding levee, but is then self-repaired by cooling of the lava that fills the breach. The lava terraces on the flanks of most of these seamounts are built in a similar fashion, although they are probably fed by tubes from the central lava pond.

[52] Finally, if these seamounts were ever eroded at the sea surface there would be a positive correlation between the depth of the summit plateaus and their ages. There is not. For example, Patton is ~2.5 m.y. older than Murray, yet its summit plateau is more than 200 m shallower than Murray's (350–400 m deep versus Murray's 600–700 m deep plateau). These two seamounts are only 145 km apart, so if Murray's summit plateau was ever at sea level, Patton's would have been as well, and would have eroded to approximately the same level.

## 5.2. Linear Versus Circular Seamount Shape

[53] Most of these seamounts display flat-topped summit plateaus and terraced or radially-ridged flank morphologies, pointing toward similar evolutionary mechanisms. Bowie and Dickins are the exceptions, as they have more linear, ridge-like morphologies, suggesting a differing volcanic style. If seamount volcanism initiates at a crustal weakness, such as a fossil transform fault, the initial volcanism may resemble a fissure eruption, and the edifice takes on the linear shape of the weakness, but as the edifice grows and the lava conduits establish consistent pathways through the crust, eruptions may concentrate at a central point that tends to build a conical seamount. The contrasting morphologies of Dickins and the nearby Denson are prime examples of these variations in volcanic style. Dickins is a linear ridge approximately parallel to regional fracture zones. It may represent a snapshot of the early history of conical seamounts such as the nearby Denson. *Davis et al.* [2002] suggested that the linear nature of seamounts along the California margin is the result of eruptions along abandoned spreading ridges in regions of complex tectonics. The spreading fabric in the Gulf of Alaska is oriented north-south, so this exact interpretation does not apply to Dickins or Bowie, but similar crustal weaknesses, such as transforms and fracture zones which are found to control seamount morphology elsewhere [e.g., *Lourenco et al.*, 1998], are at the appropriate orientation to explain Dickins and Bowie.

## 5.3. Slope Failures

[54] Like volcanic islands and terrestrial volcanoes, seafloor imaging surveys have shown that the flanks of seamounts can become unstable and fail in either a continuous "shedding" manner, or as a larger more coherent landslide [e.g., *Holcomb and*

*Searle*, 1991; *Watts and Masson*, 2001; *Moore and Clague*, 2002; *Oehler et al.*, 2004; *Mitchell*, 2003]. The visual evidence of such slope failures on the flanks of volcanic oceanic islands includes U-shaped head scarps, embayments or amphitheaters [*Malahoff*, 1987; *Mitchell*, 2003], longitudinal flow structures and transverse pressure ridges in debris avalanche structures [*Watts and Masson*, 2001], topographically depressed elongate chutes, and debris fields at the base of slope characterized by blocky and hummocky irregular topography [*Moore et al.*, 1989].

[55] Most of the seamounts described above, especially those lacking the well-developed lava-terraced morphologies, show flank and summit features suggestive of varying amounts of post-eruptive modification as seen on other oceanic islands and seamounts. That said, while many of these seamounts show various amounts of embayment of their summit plateaus, there appears to be no simple correlation between seamount age and summit area. With the exception of Denson, for reasons discussed below, there does appear to be a gross correlation between seamount age and flank morphology for the conical seamounts. Flanks of the older seamounts tend to have more of the radial-chutes-and-ridges morphology, and less of the lava-terraces-and-cones morphology. This is thought to be a result of ongoing slope failure processes that modify or completely destroy lava terraces and cones and create debris chutes separated by ridges radiating from the summit plateau, producing a stellate-type morphology [*Vogt and Smoot*, 1984; *Mitchell*, 2001]. Notice, for example, the abundance of chutes on older seamounts such as Patton, Codman, and Murray, versus the abundance of lava terraces on Warwick. Denson is an exception to these observations, in that it retains an abundance of lava terraces, despite being similar in age to failure-modified seamounts such as Pratt and Welker. Denson is also exceptional amongst these seamounts in that it was built on the youngest crust (<1–3 m.y. old at the time the seamount formed) of any of these seamounts, except for the Cobb, which is adjacent to the spreading ridge. Young crust with thin sediment cover may provide a more solid foundation for the flanks of the seamount, so that the piles of lava that make up the flanks are better coupled to the underlying crust. In contrast, seamounts that erupt onto older crust with thicker sediments are built on this layer of loosely consolidated sediments that are prone to failure, thus undermining the stability of the seamount's flanks.

[56] Although the mechanisms controlling the progressive failure of the seamount slopes are currently unknown, one possibility for these seamounts may be the presence or absence of low strength layers such as extensive hyaloclastite deposits and other hydrothermally altered zones [e.g., *Lopez and Williams*, 1993]. Several samples of hyaloclastite were recovered from the slopes of these seamounts (R. Keller et al., manuscript in preparation, 2007). The inherent weakness of these clay-altered zones and increased pore fluid within the rock mass have been shown to be an important cause of at least some volcanic island landslides [*Duffield et al.*, 1982; *Garcia and Davis*, 2001; *Oehler et al.*, 2004]. Continuing slope failures may, over time, expose additional low-strength layers allowing for the continuous "shedding" of material over the entire posteruptive life of these seamounts.

[57] Many seamounts and volcanic islands in other parts of the world that show evidence for slope failures have distinct debris fields at the bases of the affected slopes [e.g., *Clouard et al.*, 2001; *J. R. Smith et al.*, 2002; *Mitchell*, 2003; *Oehler et al.*, 2004]. There is little evidence for debris fields surrounding the Gulf of Alaska seamounts evident from these new data or data from previous surveys [e.g., *Carlson et al.*, 1996]. This may be due to a combination of the small magnitude of slope failures, high sediment deposition rates, and local erosion by migrating sea channels. Among these mechanisms, the high-rate and volume of sediment deposition in the Gulf of Alaska associated with the Surveyor and Baranof fans provide the most reasonable explanation. *Weeks et al.* [1995] determined from ODP Site 887 that as much as 270 m of sediment has been deposited on the abyssal plain near Patton Seamount over the last 18 Ma (30 m/m.y rate for the 0–6 Ma period), while *Piper et al.* [1973] determined a 175 m/m.y. sedimentation rate for the last 0.6 m.y at DSDP Site 178 in the eastern Alaskan Abyssal Plain, and *Ness* [1972] determined a 24.3 ± 0.3 m/m.y. sediment accumulation rate for the central Alaskan Abyssal Plain. These extremely high sedimentation rates are enough to mask all but the largest debris fields.

## 6. Conclusions

[58] Full coverage multibeam bathymetry maps of 12 seamounts within the Kodiak-Bowie and Cobb Seamount chains within the Gulf of Alaska show that in most cases these features share similar morphologies, characteristic of their origins at

relatively unchanging hot spots over the last 30 Ma. Of the 12, only Dickins and Bowie seamounts show morphologies that diverge from the dominant flat-topped, step-bench morphology.

[59] The varied volcanic morphology of the seamounts in the Gulf resulting from the different tectonic and volcanic environments provides a detailed picture into the stages of seamount evolution. The region is dominated by seamounts with flat summit plateaus and overall step-flat morphology, chiefly the result of repeated phases of lava pond creation, filling, breaching and overtopping, and solidification. The mildly productive Bowie and Cobb hot spots would provide the necessary long-lived point-source conditions to meet the requirement for edifice construction in this manner. Ely Seamount in the Kodiak-Bowie chain with its distinctive summit crater and well-defined flank lava ponds provides an excellent example of the initial phase of seamount development. While sea level erosion is an important process in the development of flat summit plateaus of seamounts and guyots in other locations, in the Gulf of Alaska it is the lava-pond volcanic construction style, which appears to be the primary mechanism for formation of these summit features.

[60] There is evidence to support the assertion that slope failures play an important role in the shaping of the overall morphology of each seamount, but characteristic debris lobes at the base of seamount slopes are uncommon, due to the possibility of small, but numerous slope failures, the high sedimentation rates, and the influence of the large deep-sea fan and channel systems within the Gulf of Alaska. While definitive timing of individual failure episodes is unknown, a positive correlation between seamount age and the abundance of flank failures suggest that flank modification processes continue long after volcanic activity ceases.

## Acknowledgments

[61] This research was funded by a grant from the West Coast and Polar Region National Undersea Research Center at the University of Alaska and by NOAA Ocean Exploration grants NA16RP2639 and NA04OAR4600046. We thank the captains, crews, DSV *Alvin* teams, and shipboard scientific parties of R/V *Atlantis* cruises AT3-36, AT7-15, AT7-16, and AT11-15, and Susan Merle and Andra Bobbitt for their work on surveying Cobb Seamount. Thanks also go to David Clague and two anonymous reviewers for thorough and helpful reviews, which improved the manuscript.

## References

Allan, J. F., R. L. Chase, B. Cousens, P. J. Michael, M. P. Gorton, and S. D. Scott (1993), The Tuzo Wilson volcanic field, NE Pacific: Alkaline volcanism at a complex, diffuse, transform-trench-ridge triple junction, *J. Geophys. Res.*, *98*(B12), 22,367–22,387.

Atwater, T., and J. Severinghaus (1989), Tectonic maps of the northeast Pacific, in *The Eastern Pacific Ocean and Hawaii: The Geology of North America*, vol. N, edited by E. L. Winter et al., pp. 15–20 and Plates 3A, 3B, and 3C, Geol. Soc. Am., Boulder, Colo.

Batiza, R., and D. Vanko (1984), Volcanic development of small oceanic central volcanoes on the flanks of the East Pacific Rise inferred from narrow beam echo-sounder surveys, *Mar. Geol.*, *54*, 53–90.

Bobbitt, A. M., S. G. Merle, P. J. Steinker, and R. P. Dziak (2000), Full-coverage multibeam bathymetry of Cobb and Brown Bear Seamounts, northeast Pacific Ocean, *Eos Trans. AGU*, *81*(48), Fall Meet. Suppl., Abstract V52C-06.

Budinger, T. F. (1967), Cobb Seamount, *Deep Sea Res. Oceanogr. Abstr.*, *14*, 191–201.

Caress, D. W., and D. N. Chayes (1996), Improved processing of Hydrosweep DS multibeam data on the R/V Maurice Ewing, *Mar. Geophys. Res.*, *18*, 631–650.

Carlson, P. R., A. J. Stevenson, T. R. Bruns, D. M. Mann, and Q. Huggett (1996), Sediment pathways in Gulf of Alaska from beach to abyssal plain, in *Geology of the United States' Seafloor: The View From GLORIA*, edited by J. V. Gardner et al., pp. 255–277, Cambridge Univ. Press, New York.

Chase, R. L. (1977), J. Tuzo Wilson Knolls: Canadian hotspot, *Nature*, *266*, 344–346.

Chase, T. E., H. W. Menard, and J. Mammericks (1970), Bathymetry of the North Pacific, charts 1–10, Scripps Inst. of Oceanogr., Univ. of Calif., La Jolla.

Clague, D. A., J. G. Moore, and J. R. Reynolds (2000a), Formation of submarine flat-topped volcanic cones in Hawaii, *Bull. Volcanol.*, *62*, 214–233.

Clague, D. A., J. R. Reynolds, and A. S. Davis (2000b), Near-ridge seamount chains in the northeastern Pacific Ocean, *J. Geophys. Res.*, *105*(B7), 16,541–16,561.

Clouard, V., and A. Bonneville (2005), Ages of seamounts, islands, and plateaus of the Pacific Plate, in *Plates, Plumes, and Paradigms*, edited by G. R. Foulger et al., *Spec. Pap. Geol. Soc. Am.*, *388*, 71–90.

Clouard, V., A. Bonneville, and P.-Y. Gillot (2001), A giant landslide on the southern flank of Tahiti Island, French Polynesia, *Geophys. Res. Lett.*, *28*(11), 2253–2256.

Cousens, B. L. (1996), Depleted and enriched upper mantle sources for basaltic rocks from diverse tectonic environments in the northeast Pacific Ocean: The generation of oceanic alkaline vs. tholeiitic basalts, in *Earth Processes: Reading the Isotopic Code*, *Geophys. Monogr. Ser.*, vol. 95, edited by A. Basu and S. Hart, pp. 207–231, AGU, Washington, D. C.

Cousens, B., J. Dostal, and T. S. Hamilton (1999), A near-ridge origin for seamounts at the southern terminus of the Pratt-Welker Seamount Chain, northeast Pacific Ocean, *Can. J. Earth Sci.*, *36*, 1021–1031.

Crough, S. T. (1978), Thermal origin of mid-plate hot-spot swells, *Geophys. J. R. Astron. Soc.*, *55*, 451–469.

Dalrymple, G. B., D. A. Clague, T. L. Vallier, and H. W. Menard (1987), $Ar^{40}/Ar^{39}$ age, petrology and tectonic significance of some seamounts in the Gulf of Alaska, in *Seamounts, Islands, and Atolls*, *Geophys. Monogr. Ser.*,

vol. 43, edited by B. Keating et al., pp. 297–315, AGU, Washington, D. C.

Davis, A. S., D. A. Clague, W. A. Bohrson, G. B. Dalrymple, and H. G. Greene (2002), Seamounts at the continental margin of California: A different kind of oceanic intraplate volcanism, *Geol. Soc. Am. Bull.*, *114*, 316–333.

Desonie, D. L., and R. A. Duncan (1990), The Cobb-Eikelberg seamount chain: Hotspot volcanism with mid-ocean ridge basalt affinity, *J. Geophys. Res.*, *95*(B8), 12,697–12,711.

Detrick, R. S., and S. T. Crough (1978), Island subsidence, hot spots, and lithospheric thinning, *J. Geophys. Res.*, *83*(B3), 1236–1244.

Duffield, W. A., L. Stieljes, and J. Varet (1982), Huge landslide blocks in the growth of Piton de la Fournaise, La Reunion, and Kilauea volcano, Hawaii, *J. Volcanol. Geotherm. Res.*, *12*, 147–160.

Eakins, B. W., and J. E. Robinson (2006), Submarine geology of Hana Ridge and Haleakala Volcano's northeast flank, Maui, *J. Volcanol. Geotherm. Res.*, *151*, 229–250.

Fornari, D. J., M. R. Perfit, J. F. Allan, R. Batiza, R. Haymon, A. Barone, W. B. F. Ryan, T. Smith, Simkin, and M. A. Luckman (1988), Geochemical and structural studies of the Lamont Seamounts: Seamounts as indicators of mantle processes, *Earth Planet. Sci. Lett.*, *89*, 63–83.

Garcia, M. O., and M. G. Davis (2001), Submarine growth and internal structure of ocean island volcanoes based on submarine observations of Mauna Loa volcano, Hawaii, *Geology*, *29*, 163–166.

Gardner, J. V., and L. A. Mayer (2005), U.S. Law of the Sea cruise to map the foot of the slope and 2500-m isobath of the Gulf of Alaska continental margin, CRUISES KM0514-1 and KM0514-2, *CCOM/JHC Admin. Rep. 05-1*, 111 pp., Cent. for Coastal and Ocean Mapp./Joint Hydrogr. Cent., Durham, N. H.

Hegner, E., and M. Tatsumoto (1989), Pb, Sr, and Nd isotopes in seamount basalts from the Juan de Fuca Ridge and Kodiak-Bowie Seamount Chain, Northeast Pacific, *J. Geophys. Res.*, *94*(B12), 17,839–17,846.

Herlihy, D. R. (2000), Descriptive report to accompany hydrographic surveys H10996 & H10999, Proj. OPR-S-O909-RA-002 Bowie Seamount, 30 pp., Natl. Oceanic and Atmos. Admin., Silver Spring, Md.

Holcomb, R. T., and R. C. Searle (1991), Large landslides from oceanic volcanoes, *Mar. Geotechnol.*, *10*, 19–32.

Hurley, R. J. (1960), The geomorphology of abyssal plains in the northeast Pacific Ocean, *Ref. 60-7*, 105 pp., Scripps Inst. of Oceanogr., La Jolla, Calif.

Keller, R. A., M. R. Fisk, R. A. Duncan, and W. M. White (1997), 16 m.y. of hotspot and nonhotspot volcanism on the Patton-Murray seamount platform, Gulf of Alaska, *Geology*, *25*, 511–514.

Lajoie, K. R. (1986), Coastal tectonics, in *Active Tectonics*, *Studies in Geophysics Series, Geophysics Research Forum*, edited by R. Wallace, pp. 95–124, Natl. Acad., Washington, D. C.

Lambeck, K. C., L. Penney, S. M. Nakiboglu, and R. Coleman (1984), Subsidence and flexure along the Pratt-Welker seamount chain, *J. Geodyn.*, *1*, 29–60.

Lonsdale, P. (1989), A geomorphological reconnaissance of the submarine part of the submarine part of the East Rift Zone of Kilauea Volcano, Hawaii, *Bull. Volcanol.*, *51*, 123–144.

Lopez, D. L., and S. T. Williams (1993), Catastrophic volcanic collapse: Relation to hydrothermal processes, *Science*, *260*, 1794–1796.

Lourenco, N., J. M. Miranda, J. F. Luis, A. Ribeiro, L. A. Mendes Victor, J. Madeira, and H. D. Needham (1998), Morpho-tectonic analysis of the Azores volcanic plateau from a new bathymetric compilation of the area, *Mar. Geophys. Res.*, *20*, 141–156.

Malahoff, A. (1987), Geology of the summit of Loihi submarine volcano, *U. S. Geol. Surv. Prof. Pap.*, *1350*, 133–144.

Mitchell, N. C. (2001), Transition from circular to stellate forms of submarine volcanoes, *J. Geophys. Res.*, *106*(B2), 1987–2003.

Mitchell, N. C. (2003), Susceptibility of mid-ocean ridge volcanic islands and seamounts to large-scale landsliding, *J. Geophys. Res.*, *108*(B8), 2397, doi:10.1029/2002JB001997.

Moore, J. G., and D. A. Clague (2002), Mapping the Nuuanu and Wailau landslides in Hawaii, in *Hawaiian Volcanoes: Deep Underwater Perspectives*, *Geophys. Monogr. Ser.*, vol. 128, edited by E. Takahashi et al., pp. 223–244, AGU, Washington, D. C.

Moore, J. G., D. A. Clague, R. T. Holcomb, P. W. Lipman, W. R. Normark, and M. E. Torresan (1989), Prodigious submarine landslides on the Hawaiian Ridge, *J. Geophys. Res.*, *94*(B12), 17,465–17,484.

Morgan, J. W. (1972), Deep mantle convective plumes and plate motions, *Am. Assoc. Petrol. Geol. Bull.*, *56*, 201–213.

Ness, G. E. (1972), The structure and sediments of Surveyor Deep-Sea Channel, M. S. thesis, 77 pp., Oreg. State Univ., Corvallis.

Ness, G. E., and L. D. Kulm (1973), Origin and development of Surveyor Deep-Sea Channel, *Geol. Soc. Am. Bull.*, *84*, 3339–3354.

Oehler, J.-F., P. Labazuy, and J.-F. Lenat (2004), Recurrence of major flank landslides during the last 2-Ma—History of Reunion Island, *Bull. Volcanol.*, *66*, 585–598.

Paduan, J. B., D. A. Clague, and A. S. Davis (2004), Evidence that three seamounts off southern California were ancient islands, *Eos Trans. AGU*, *85*(47), Fall Meet. Suppl., Abstract V43E-1463.

Piper, D. J. W., R. von Huene, and J. R. Duncan (1973), Late Quaternary sedimentation in the active eastern Aleutian Trench, *Geology*, *1*, 19–22.

Schwartz, M. L. (1972), Seamounts as sea-level indicators, *Geol. Soc. Am. Bull.*, *83*, 2975–2980.

Schwartz, M. L., and K. L. Lingbloom (1973), Research submersible reconnaissance of Cobb seamount, *Geology*, *1*, 31–32.

Silver, E. A., R. von Huene, and J. K. Crouch (1974), Tectonic significance of the Kodiak-Bowie Seamount chain, northeastern Pacific, *Geology*, *2*, 147–150.

Smith, D. K., L. S. L. Kong, K. T. M. Johnson, and J. R. Reynolds (2002), Volcanic morphology of the submarine Puna Ridge, Kilauea Volcano, in *Hawaiian Volcanoes: Deep Underwater Perspectives*, *Geophys. Monogr. Ser.*, vol. 128, edited by E. Takahashi et al., pp. 125–142, AGU, Washington, D. C.

Smith, J. R., K. Satake, J. K. Morgan, and P. W. Lipman (2002), Submarine landslides and volcanic features on Kohala and Mauna Kea volcanoes and the Hana Ridge, Hawaii, in *Hawaiian Volcanoes: Deep Underwater Perspectives*, *Geophys. Monogr. Ser.*, vol. 128, edited by E. Takahashi et al., pp. 11–28, AGU, Washington, D. C.

Smith, W. H. F., and D. T. Sandwell (1997), Global seafloor topography from satellite altimetry and ship depth soundings, *Science*, *277*, 1957–1962.

Smoot, N. C. (1981), Multi-beam sonar surveys of guyots of the Gulf of Alaska, *Mar. Geol.*, *43*, M87–M94.

Smoot, N. C. (1985), Observations on Gulf of Alaska seamount chains by multi-beam sonar, *Tectonophysics*, *115*, 235–246.

Stevenson, A. J., and R. W. Embley (1987), Deep-sea fan bodies, terrigenous turbidite sedimentation, and petroleum geology, Gulf of Alaska, in *Geology and Resource Potential of the Continental Margin of Western North America and Adjacent Ocean Basins, Beaufort Sea to Baja California*, *Earth Sci. Ser.*, vol. 6, edited by D. W. Scholl, pp. 503–522, Circum-Pac. Counc. for Energy and Miner. Resour., Houston, Tex.

Turner, D. L., R. B. Forbes, and C. W. Naeser (1973), Radiometric ages of Kodiak seamount and Giacomini guyot, Gulf of Alaska: Implications for circum-Pacific tectonics, *Science*, *182*, 579–581.

Turner, D. L., R. D. Jarrard, and R. B. Forbes (1980), Geochronology and origin of the Pratt-Welker seamount chain, Gulf of Alaska: A new pole of rotation for the Pacific Plate, *J. Geophys. Res.*, *85*, 6547–6556.

Vogt, P. R., and N. C. Smoot (1984), The Giesha Guyots: Multibeam bathymetry and morphometric interpretation, *J. Geophys. Res.*, *89*(B13), 11,085–11,107.

Watts, A. B., and D. G. Masson (2001), New sonar evidence for recent catastrophic collapses on the north flank of Tenerife, Canary Islands, *Bull. Volcanol.*, *63*, 8–19.

Weeks, R. J., A. P. Roberts, K. L. Verosub, M. Okada, and G. J. Dubuisson (1995), Magnetostratigraphy of upper Cenozoic sediments from Leg 145, North Pacific Ocean, *Proc. Ocean Drill. Program Sci. Results*, *145*, 491–521.

Wessel, P., Y. Harada, and L. W. Kroenke (2006), Toward a self-consistent, high-resolution absolute plate motion model for the Pacific, *Geochem. Geophys. Geosyst.*, *7*, Q03L12, doi:10.1029/2005GC001000.

Wilson, J. T. (1963), A possible origin of the Hawaiian Islands, *Can. J. Phys.*, *41*, 863–870.

Wilson, L., and E. A. Parfitt (1993), The formation of perched lava ponds on basaltic volcanoes: The influence of flow geometry on cooling-limited lava flow lengths, *J. Volcanol. Geotherm. Res.*, *56*, 113–123.

Winterer, E. L. (1989), Sediment thickness map of the Northeast Pacific, in *The Eastern Pacific Ocean and Hawaii: The Geology of North America*, vol. N, edited by E. L. Winter et al., pp. 307–310, Geol. Soc. Am., Boulder, Colo.